© 2021. Published by The Company of Biologists Ltd | Journal of Experimental Biology (2021) 224, jeb238816. doi:10.1242/jeb.238816

RESEARCH ARTICLE

Characterization of *Halyomorpha halys* TAR1 reveals its involvement in (*E*)-2-decenal pheromone perception

Luca Finetti[1], Marco Pezzi[1], Stefano Civolani[1,2], Girolamo Calò[3], Chiara Scapoli[1] and Giovanni Bernacchia[1,*]

ABSTRACT

In insects, tyramine receptor 1 (TAR1) has been shown to control several physiological functions, including olfaction. We investigated the molecular and functional profile of the *Halyomorpha halys* type 1 tyramine receptor gene (*HhTAR1*) and its role in olfactory functions of this pest. Molecular and pharmacological analyses confirmed that the *HhTAR1* gene codes for a true TAR1. RT-qPCR analysis revealed that *HhTAR1* is expressed mostly in adult brain and antennae as well as in early development stages (eggs, 1st and 2nd instar nymphs). In particular, among the antennomeres that compose a typical *H. halys* antenna, *HhTAR1* was more expressed in flagellomeres. Scanning electron microscopy investigation revealed the type and distribution of sensilla on adult *H. halys* antennae: both flagellomeres appear rich in trichoid and grooved sensilla, known to be associated with olfactory functions. Through an RNAi approach, topically delivered *HhTAR1* dsRNA induced a 50% downregulation in gene expression after 24 h in *H. halys* 2nd instar nymphs. An innovative behavioural assay revealed that *HhTAR1* RNAi-silenced 2nd instar nymphs were less susceptible to the alarm pheromone component (*E*)-2 decenal as compared with controls. These results provide critical information concerning the role of TAR1 in olfaction regulation, especially alarm pheromone reception, in *H. halys*. Furthermore, considering the emerging role of TAR1 as target of biopesticides, this work opens the way for further investigation on innovative methods for controlling *H. halys*.

KEY WORDS: Brown marmorated stink bug, TAR1 receptor, Antennae, Olfaction, Behaviour, RNAi

INTRODUCTION

Identifying volatile compounds through the olfactory system allows insects to find food sources, avoid predators and localize putative partners and oviposition habitats (Gadenne et al., 2016). Furthermore, olfactory modulation by volatile molecules with repellent activity could be a promising strategy for pest control (Carey and Carlson, 2011). The basic organization of the olfactory system begins with the antennae, organs possessing cuticular structures, the sensilla, innervated by olfactory sensory neurons (OSNs) (Amin and Lin, 2019). The OSNs recognize different molecules through special olfactory receptors. Each OSN expresses only one type of olfactory receptor, ensuring the specificity of signal for a single odour (Zhao and McBride, 2020). When an OSN is activated, it sends the output signal through the axon to the antennal lobe. Here, excitatory projection neurons (PNs) transport the olfactory information to brain centres such as the mushroom body and the lateral horn (Tanaka et al., 2012). The mushroom body plays an important role in olfactory learning and memory (Caron et al., 2013) whereas the lateral horn controls innate olfactory response functions (Jefferis et al., 2007). In insects, the olfactory system can be modulated by exogenous (photoperiod, temperature) and endogenous (hormones) factors.

The biogenic amines tyramine (TA) and octopamine (OA) are present in high levels in the nervous tissue of insects, suggesting a role as neurotransmitters (Roeder, 2005). Furthermore, TA and OA act also as neurohormones and neuromodulators in a wide variety of physiological processes, acting in a paracrine, endocrine and autocrine way on the cells of the organism (Pauls et al., 2018).

Initially, TA was considered only as a biosynthetic intermediate of OA (Lange, 2009), but later numerous studies showed that TA is indeed an important neurotransmitter (Blenau and Baumann, 2003; Roeder, 2005, 2020; Lange, 2009). Among invertebrates, TA is the endogenous agonist of the tyramine receptors (TARs). Structurally, TARs are part of the superfamily of G protein-coupled receptors (GPCR) sharing a typical structure with seven transmembrane domains (Ohta and Ozoe, 2014). Several studies have highlighted that TARs can by coupled with both G_q (increasing intracellular calcium levels) and G_i proteins (decreasing cAMP levels) (Saudou et al., 1990; Blenau et al., 2000; Enan, 2005; Rotte et al., 2009). Based on the rank order of potency of agonists, TARs have been classified into three different types (Wu et al., 2014): TAR1, coupled with G_q and G_i proteins, and TAR2, coupled only with G_i protein, while TAR3 has so far been described only in *Drosophila melanogaster* (Bayliss et al., 2013; Wu et al., 2014). The first TAR1 was characterized in *D. melanogaster* (Saudou et al., 1990). The receptor, called Tyr-dro, showed higher affinity (12-fold) for TA than for OA and was mainly expressed in the heads. Since then the same receptor has been characterized in several orders of insects: Hymenoptera (Blenau et al., 2000), Orthoptera (Poels et al., 2001), Lepidoptera (Ohta et al., 2003), Hemiptera (Hana and Lange, 2017a) and Diptera (Finetti et al., 2020).

Several physiological and behavioural functions are controlled by TAR1, including olfaction. Kutsukake and colleagues (2000) characterized *honoka*, a *D. melanogaster* strain that presented a TAR1 mutation and a compromised olfactory profile. These insects were not able to localize repellent stimuli, suggesting that TAR1 could be involved in this physiological response. Furthermore, RNAi-mediated modulation of TAR1 expression was shown to affect the gregarious and solitary phase change of locusts through a different olfactory sensibility to attractive and repulsive volatiles (Ma et al., 2015). In honeybee antennae, an upregulation of TAR1 was observed during the transition from nurses to pollen foragers, suggesting TAR1 regulation of their behavioural plasticity (McQuillan et al., 2012). High TAR1 levels were also found in

[1]Department of Life Sciences and Biotechnology, University of Ferrara, 44121 Ferrara, Italy. [2]InnovaRicerca s.r.l. Monestirolo, 44124 Ferrara, Italy. [3]Department of Biomedical and Specialty Surgical Sciences, Section of Pharmacology, University of Ferrara, 44121 Ferrara, Italy.

*Author for correspondence (bhg@unife.it)

L.F., 0000-0001-5558-9156; G.B., 0000-0002-3259-7273

Received 5 October 2020; Accepted 2 March 2021

the antennae of *Mamestra brassicae* and *Agrotis ipsilon*, further suggesting a pivotal role of this receptor in olfactory modulation (Brigaud et al., 2009; Duportets et al., 2010).

TAR1s are considered an interesting target for insecticides, especially bioinsecticides. Amitraz is an acaricide and non-systemic insecticide that targets the OA receptors. However, recent studies have shown that Amitraz can also exert its toxic effect through TAR1 activation (Wu et al., 2014; Kumar, 2019). Furthermore, a secondary metabolite of Amitraz, BTS-27271, increases the TA response of the *Rhipicephalus microplus* TAR1 (Gross et al., 2015). Concerning biopesticides, in recent years several studies have shown that monoterpenes could interact and activate, directly or indirectly, TAR1s. Enan (2005) was the first to describe an agonist effect of several monoterpenes (thymol, carvacrol, α-terpineol, eugenol) on the *D. melanogaster* TAR1. However, the same monoterpenes did not show the same pharmacological profile in *Drosophila suzukii* and *R. microplus* TAR1 receptors, where they act as positive allosteric modulators (Gross et al., 2017; Finetti et al., 2020).

Halyomorpha halys (Rhyncota; Pentatomidae), an insect typical of Eastern Asia (China, Japan, Taiwan and Korea) (Haye et al., 2015), was detected for the first time in the USA in 1998 (Hoebeke and Carter, 2003) and has become a stable presence in orchards since 2010 (Rice et al., 2014). Its first European appearance was reported in 2004 in Switzerland, leading to its spread across the continent (Cesari et al., 2018). *Halyomorpha halys* is responsible for major damage to many economically relevant crops (Leskey and Nielsen, 2018). The damage is caused by the perforation of the external integuments of fruits by the rostrum, the specialized sucking apparatus typical of Rhyncota. This causes necrotic areas on fruits, as well as the transmission of other phytopathogens, leading to a significant decrease in the product value (Peiffer and Felton, 2014). In Asiatic regions, the life cycle of *H. halys* consists of only one generation per year (Lee et al., 2013). However, in warmer regions, the insect is able to complete up to four annual generations, significantly increasing its number in the area (each female is able to lay between 100 and 500 eggs per cycle) (Nielsen et al., 2016). This relevant pest shows high resistance to common pesticides, making difficult its control and elimination (Bergmann and Raupp, 2014).

The present work aimed to characterize the *H. halys* TAR1. Based on studies performed in *D. melanogaster* (Kutsukake et al., 2000), *M. brassicae* (Brigaud et al., 2009) and *Apis mellifera* (Mustard et al., 2005; Thamm et al., 2017; Sinakevitch et al., 2017), we advanced the hypothesis that the *H. halys* TAR1 could be involved in olfactory perception. First, we identified and characterized the *H. halys* TAR1 (*HhTAR1*) gene. Then, we tested the ability of RNAi *HhTAR1*-mediated downregulated insects to respond to the alarm pheromone (*E*)-2-decenal compared with control insects. These findings may shed light on the importance of TAR1 in *H. halys* pheromone perception and contribute to developing new TAR1-targeting control tools.

MATERIALS AND METHODS

Insects and reagents

Individuals of *Halyomorpha halys* Stål 1855 were reared on green beans and kiwi with a photoperiod of 16 h light:8 h dark, at a temperature of 24±1°C. Tyramine hydrochloride, octopamine hydrochloride, yohimbine hydrochloride, γ-aminobutyric acid, serotonin hydrochloride, adrenaline (epinephrine), noradrenaline (norepinephrine), L-DOPA, Brilliant Black, bovine serum albumin (BSA), Hepes and (*E*)-2-decenal were all obtained from Sigma-Aldrich (St Louis, MO, USA). Dopamine was obtained from Tocris Bioscience (Bristol, UK). Pluronic acid and fluorescent dye Fluo-4 AM were purchased from Thermo Fisher Scientific (Waltham, MA, USA). All compounds were dissolved in dimethyl sulfoxide (10 mmol l^{-1}) and stock solutions were kept at −20°C until use. Serial solutions were made in the assay buffer: Hanks' Balanced Salt solution (HBSS)/Hepes 20 mmol l^{-1} buffer, containing 0.01% BSA and 0.1% DMSO.

Isolation and cloning of full-length *HhTAR1*

Sequence alignment by BLASTN performed with the orthologous gene *RpTAR1* (GenBank accession no. MF377527.1; Hana and Lange, 2017a) from *Rhodnius prolixus* suggested that the putative transcript (GenBank accession no. XM_014422850.2) predicted in the *H. halys* genome project (GenBank accession no. PRJNA298780) may code for a putative HhTAR1 (GenBank accession no. XP_014278336.1).

Total RNA was extracted from four *H. halys* adults using RNAgent® Denaturing Solution (Promega, Madison, WI, USA), quantified in a micro-volume spectrophotometer (Biospec-Nano, Shimadzu, Kyoto, Japan) and analysed by 0.8% w/v agarose gel electrophoresis. A 1 µg sample of RNA was treated with DNase I (Thermo Fisher Scientific) and used for the synthesis of cDNA, carried out with the OneScript® Plus cDNA Synthesis Kit (ABM, Richmond, BC, Canada). For amplification of the full *HhTAR1* open reading frame (ORF), specific primers were designed based on the annotated transcript (XM_014422850.2). The Kozak translation initiation sequence (GCCACC) was inserted at the 5′ end of the receptor (Table 1). High fidelity amplification was achieved using Herculase II Fusion DNA Polymerase (Agilent, Santa Clara, CA, USA) and a touchdown thermal profile: predenaturation at 95°C for 3 min, followed by 10 cycles at 95°C for 20 s, 65–55°C for 20 s (minus 1°C/cycle), 68°C for 2 min, 30 cycles at 95°C for 20 s, 55°C for 20 s, 68°C for 2 min and a final extension at 68°C for 4 min. The PCR product was gel purified by Illustra GFX PCR DNA and Gel Band Purification Kits (GE Healthcare, Chicago, IL, USA), cloned into pJET 1.2/blunt vector (Thermo Fisher Scientific) and transformed into *Escherichia coli* SIG10 5-α Chemically Competent Cells (Sigma-Aldrich). Positive clones were selected using LB broth agar plates with 100 µg ml^{-1} ampicillin. Plasmid

Table 1. Primers used in this study

Primer	Primer sequence (5′–3′)
Cloning	
HhTAR1-Fw	TTAGTGCGGTGAGGAAGGTT
HhTAR1-Fw-Kozak	GCCACCATGGAGTGGGACTATAGAG
HhTAR1-Rev	CGATTTTCATGGAGAAGTGGA
RT-qPCR analysis	
HhTAR1-Fw	CTCATTGGCTGGAACGACTG
HhTAR1-Rev	CCCGTTCACGTAACCTCCTC
ARP8-Fw	TTGATGCTGACTGGCCCTAA
ARP8-Rev	GGCCTCCTTCGTTGGTACAG
UBE4A-Fw	CGCCAGCTGACTTTTCCTCT
UBE4A-Rev	GACAGCAGTGGCTCCATCAG
dsRNA synthesis	
HhTAR1-Fw	GAATTAATACGACTCACTATAGGGAGACCGGAAGTCTTCAGCAACT
HhTAR1-Rev	GAATTAATACGACTCACTATAGGGAGACGTGACTTAGGGGAATTGG
LacZ-Fw	GAATTAATACGACTCACTATAGGGAGATGAAAGCTGGCTACAGGA
LacZ-Rev	GAATTAATACGACTCACTATAGGGAGAGCAGGCTTCTGCTTCAAT

was then extracted by GenElute™ Plasmid Miniprep Kit (Sigma-Aldrich) and verified by DNA sequencing (BMR Genomics, Padua, Italy). The sequence, named *HhTAR1*, was deposited in GenBank with the accession number MT513133. For expression in HEK 293 cells, the ORF of *HhTAR1* was excised from the pJET 1.2 vector and inserted into the pcDNA 3.1 (+) Hygro expression vector using Xho I and Xba I restriction sites.

Molecular characterization of HhTAR1

Molecular characterization of the predicted HhTAR1 was carried out using TMHMM v.2.0. and the Kyte and Doolittle (1982) method. The 3D model was analysed by SWISSMODEL and MolProbity. Multiple protein sequence alignments between the deduced amino acid sequence of HhTAR1 and other type 1 TAR sequences were performed using Clustal Omega (https://www.ebi.ac.uk/Tools/msa/clustalo/) and BioEdit Sequence Alignment Editor 7.2.6.1. Phylogenetic neighbour-joining analysis was performed by MEGA software (version 7) with 1000-fold bootstrap resampling. The *D. melanogaster* GABA B receptor (GABABR) was used as an outgroup to root the tree.

Transient expression of HhTAR1 in HEK 293 cells

HEK 293 cells were grown at 37°C and 5% CO_2 in Dulbecco's modified Eagle's medium, high glucose (DMEM) supplemented with 10% fetal bovine serum (Euroclone, Milan, Italy). To prevent bacterial contamination, penicillin (100 U ml^{-1}) and streptomycin (0.1 mg ml^{-1}) were added to the medium. The cells were transiently transfected with pcDNA 3.1 (+)/*HhTAR1* in T75 cell culture flasks (Euroclone) using JetOPTIMUS (Polyplus-Transfection, New York, NY, USA), following the manufacturer's protocol. Cells were incubated in the transfection medium for 24 h under normal cell growth conditions before their use in the calcium mobilization assay.

Calcium mobilization assay

Cells were seeded at a density of 50,000 cells per well, total volume of 100 µl, into poly-D-lysine-coated 96-well black, clear-bottom plates. After 24 h incubation under normal cell culture conditions, the cells were incubated with 1× HBSS supplemented with 2.5 mmol l^{-1} probenecid, 3 µmol l^{-1} Fluo-4 AM calcium-sensitive fluorescent dye and 0.01% pluronic acid for 30 min at 37°C. After that, the loading solution was removed and 1× HBSS supplemented with 20 mmol l^{-1} Hepes, 2.5 mmol l^{-1} probenecid and 500 µmol l^{-1} Brilliant Black were added. Cell culture and drug plates were placed into a fluorometric imaging plate reader (FlexStation II, Molecular Devices, Sunnyvale, CA, USA) and fluorescence changes were measured after 10 min of stabilization at 37°C. On-line additions were carried out in a volume of 50 µl/well after 20 s of basal fluorescence monitoring. Besides TA and OA, the biogenic amines dopamine, L-DOPA, adrenaline, noradrenaline and serotonin, and the neurotransmitter γ-aminobutyric acid were tested at 100 µmol l^{-1} as putative HhTAR1 ligands. In antagonism protocols, to facilitate drug diffusion into the wells, the assays were performed at 37°C with three cycles of mixing (25 µl from each well moved up and down 3 times). Yohimbine (1 µmol l^{-1}) was added prior to measuring (25 min beforehand) the TA dose–response curve. The fluorescence readings, expressed in fluorescence intensity units (FIU), were measured every 2 s for 120 s.

Reverse transcription-quantitative PCR (RT-qPCR) analysis

Total RNA was extracted from whole bodies of *H. halys* samples at various developmental stages (n=20 eggs, n=10 1st instar nymphs, n=6 2nd or 3rd instar nymphs, n=3 4th or 5th instar nymphs or adults) and different organs (n=30 antennae, n=40 antennae regions, n=6 brains, n=6 midguts, n=12 testicles or ovaries) using RNAgent® Denaturing Solution (Promega). The organs of *H. halys* were dissected in an RNA preservation medium [20 mmol l^{-1} EDTA disodium (pH 8.0), 25 mmol l^{-1} sodium citrate, 700 g l^{-1} ammonium sulfate, final pH 5.2]. A 1 µg sample of purified RNA was then treated with DNase I (Thermo Fisher Scientific) and used for cDNA synthesis, carried out with the OneScript® Plus cDNA Synthesis Kit (ABM), according to the manufacturer's instructions. qPCR was performed using a CFX Connect Real-Time PCR Detection System (Bio-Rad) in a 12 µl reaction mixture containing 0.8 µl of cDNA (obtained above), 6 µl ChamQ SYBR qPCR Master Mix (Vazyme, Nanchino, China), 0.4 µl forward primer (10 µmol l^{-1}), 0.4 µl reverse primer (10 µmol l^{-1}) and 3.6 µl nuclease-free water. Thermal cycling conditions were: 95°C for 2 min, 40 cycles at 95°C for 15 s and 60°C for 20 s. After the cycling protocol, a melting-curve analysis from 60 to 95°C was applied. Expression of *HhTAR1* was normalized in accordance with the relative quantification method (Larionov et al., 2005) using *ARP8* and *UBE4A* as reference genes (Bansal et al., 2016). Gene-specific primers (Table 1) were used and at least three independent biological replicates, each in triplicate, were performed for each sample.

Antennae preparation and scanning electron microscopy analysis

Preliminary morphological investigations were performed on 10 *H. halys* adults (n=5 males and n=5 females) using a Nikon SMZ 800 stereomicroscope (Nikon Instruments Europe, Amsterdam, The Netherlands), provided with a Nikon Digital Sight Ds-Fil camera (Nikon Instruments Europe) and connected to a personal computer with the imaging software NIS Elements Documentation (Nikon Instruments Europe). Based on stereomicroscope observations, the head was dissected from the body and prepared for scanning electron microscopy (SEM), according to previously published procedures (Pezzi et al., 2015, 2016). Afterwards, samples were critical point dried in a Balzers CPD 030 dryer (Leica Microsystems, Wetzlar, Germany), glued on stubs, and coated with gold–palladium in an S150 Edwards sputter coater (HHV Ltd, Crawley, UK). The SEM observations were conducted at the Electron Microscopy Centre of the University of Ferrara, using a Zeiss EVO 40 SEM (Zeiss, Milan, Italy).

Synthesis of dsRNA and *H. halys* treatment

For RNAi silencing, *HhTAR1* and *LacZ* (control) amplicons, 400–500 bp long, were generated by PCR using primers with 5′ extensions containing T7 promoters (Table 1). These products were cloned into the pJET 1.2 vector (Thermo Fisher Scientific) and then used as templates for *in vitro* dsRNA synthesis performed by T7 RNA Polymerase (Jena Bioscience, Jena, Germany), according to the manufacturer's protocol. After 1 h of synthesis at 37°C, DNase I (Thermo Fisher Scientific) treatment was performed and the dsRNA was cleaned up by ammonium acetate precipitation (Rouhana et al., 2013). Finally, the dsRNA was resuspended in ultrapure water and quantified by a Biospec-Nano spectrophotometer. To induce RNAi silencing, 2nd stage *H. halys* nymphs, 3 days post-ecdysis, were treated with 100 ng of *TAR1* or *LacZ* dsRNA in 1 µl of solution using a 0.1–2 µl micropipette. The dsRNA molecules were topically delivered through a drop placed on the abdomen of nymphs (Fig. S4). Insects were tested by behavioural assay after 24 h, and the *HhTAR1* transcript level was measured by RT-qPCR, as described above.

Journal of Experimental Biology (2021) 224, jeb238816. doi:10.1242/jeb.238816

Repellency assay

An open Petri dish (90 mm×15 mm), containing 24 h starved *H. halys* 2nd instar nymphs and a green bean, was placed inside a Plexiglas box (50 cm each side) with two lateral openings covered by nets to allow air circulation. The negative control acetone or the positive repellent control (*E*)-2-decenal were applied to a filter paper (1 cm×1 cm) that was placed under the green bean. The positive control (*E*)-2-decenal, dissolved in acetone, was tested at a fixed quantity of 10 µg, a value ensuring the maximum repellence activity against the *H. halys* nymphs (Zhong et al., 2018). The number of *H. halys* nymphs standing and feeding on the green bean was monitored every 10 min for 1 h. Four biological replicates were made, each including at least 10 insects, for both untreated and dsRNA-treated *H. halys* nymphs. All experiments were performed in the morning in a behavioural room with a controlled temperature of 24±1°C.

Data analysis and terminology

All data were elaborated using Graph Pad Prism 6.0 (La Jolla, CA, USA). Data are expressed as means±s.e.m. of *n* experiments and were analysed using one- or two-way analysis of variance (ANOVA) followed by Dunnett's or Turkey's test for multiple comparison. In the pharmacological assays, the concentration–response curves were fitted using the four-parameter logistic equation:

$$\text{Effect} = \text{baseline} + \frac{(E_{\max} - \text{baseline})}{(1 + 10^{(\log EC_{50} - \log[\text{compound}]) \times H})}, \quad (1)$$

where $E_{\max}$ is the maximum response and H is the Hill slope. Agonist potency was expressed as pEC_{50}, defined as the negative logarithm to base 10 of the agonist molar concentration that produces 50% of the maximum possible effect of that agonist. Antagonist potency was derived from the Gaddum–Schild equation:

$$pA_2 = -\log \frac{CR - 1}{[\text{antagonist}]}, \quad (2)$$

assuming a slope value equal to unity, where pA_2 is the negative logarithm of the molar concentration of competitive antagonist and CR indicates the ratio between agonist potency in the presence and absence of antagonist (Kenakin, 2014).

RESULTS

Molecular characterization of HhTAR1

The amplified *HhTAR1* sequence was 1347 bp long and coded for a 449 amino acid polypeptide with a predicted MW of 50.97 kDa and pI of 9.41. In terms of structural domains, both TMHMM v.2.0 software and the Kyte and Doolittle (1982) method suggest seven putative transmembrane domains, as expected for a GPCR. The helixes are flanked by an extracellular N-terminus of 51 residues and an intracellular C-terminus of 18 residues. Furthermore, the HhTAR1 sequence contains a DRY conserved sequence in transmembrane (TM) III, several N-glycosylation sites in the extracellular N-terminus, and P-glycosylation sites, two specific for PKA and 10 specific for PKC (Fig. S1). These features are important for the correct folding and function of GPCRs (Nørskov-Lauritsen and Bräuner-Osborne, 2015). Moreover, at position 128 in TM III there is a conserved aspartic acid (D128, shown in Fig. 1A,B) responsible for the interaction with TA, the endogenous agonist of the TAR1s (Ohta and Ozoe, 2014).

To study the binding site structure, the HhTAR1 amino acid sequence was analysed by SWISS-MODEL (Waterhouse et al., 2018). The model was created based on the crystal structure of the human α2A adrenergic receptor (template code: 6kux.1.A), which shares 33.51% sequence identity with HhTAR1. The 3D model of the whole receptor and the putative ligand binding pocket are shown in Fig. 1. Several serine residues in TM V have been found to play a key role in stabilizing the interaction with TA in *Bombyx mori* (Ohta et al., 2004) and *Sitophilus oryzae* (Braza et al., 2019) TAR1. These serine residues localized in the TM V are also conserved in HhTAR1 at positions S212, S213 and S216 (Fig. 1B). MolProbity model quality investigation (Table 2) confirmed the validity of the SWISS-MODEL 3D model of HhTAR1 (Chenn et al., 2010). The HhTAR1 deduced amino acid sequence was then compared with that of several OA and TA receptors, allowing the construction of a neighbour-joining phylogenetic tree using MEGA7 (Fig. S2). As expected, HhTAR1 grouped in the TAR1 family, the main monophyletic group, and shared the highest percentage identity with the *Rhodnius prolixus* TAR1 (GenBank accession no. MF377527.1), another Rhyncota. Based on the phylogenetic results, a multiple sequence alignment was performed between the HhTAR1 deduced amino acid sequence and TAR1 from other insects (Fig. 2). The analysis further confirms the similarity of HhTAR1 to known TAR1 receptors, showing the typical

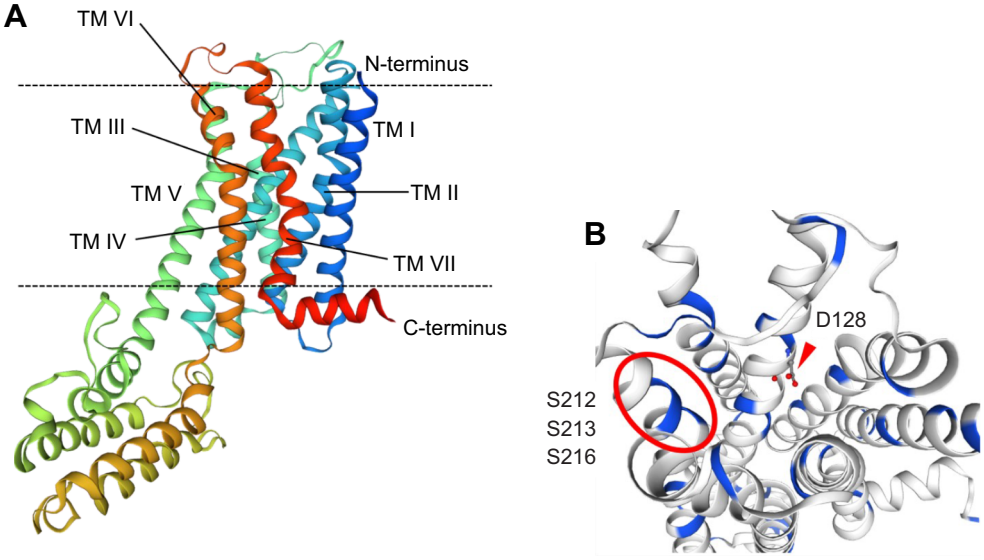

Fig. 1. Structural overview of HhTAR1. (A) Predicted structure (using SWISS-MODEL) of the whole *Halyomorpha halys* type 1 tyramine receptor (HhTAR1) showing the transmembrane (TM) domains. (B) Detail of the putative ligand binding pocket of HhTAR1, seen from the extracellular side. Serine residues are highlighted in blue. The aspartic acid in TM3 (D128) is shown by a triangle and the three serine residues interacting with tyramine (TA) are circled.

Journal of Experimental Biology (2021) 224, jeb238816. doi:10.1242/jeb.238816

Table 2. MolProbity results based on the HhTAR1 3D model obtained by SWISS-MODEL software

MolProbity parameter	Result
MolProbity score	1.95
ClashScore	3.07 (M260, K263)
Ramachandran favoured	97.94% (goal: >98%)
Ramachandran outliers	0.51% (D331, P77) (goal: <0.2%)

GPCR structure with highly conserved domains corresponding to the transmembrane regions as well as the TA binding site.

Pharmacological validation of HhTAR1

In the calcium mobilization assay, HhTAR1 was activated by both TA and OA in a concentration-dependent manner (Fig. 3A). TA evoked the release of intracellular calcium with a pEC_{50} of 5.99 (95% confidence limit 5.32–6.66) and E_{max} of 109.33±14.86 FIU, while OA was less potent, with a pEC_{50} of 4.41 (95% confidence limit 4.17–4.64) calculated assuming the TA maximum effect (Fig. 3A). In wild-type HEK 293 cells, TA and OA were completely inactive when tested in the same concentration range (from 10^{-10} to 10^{-4} mol l^{-1}; data not shown). Antagonist studies were then performed using yohimbine, the standard α2-adrenergic receptor antagonist, that was demonstrated to antagonize TAR1 in previous studies (Le Corre et al., 2004; Hana and Lange, 2017a,b; Finetti et al., 2020). When tested against HhTAR1, yohimbine was completely inactive as an agonist, whereas at 1 µmol l^{-1} it elicited a rightward shift of the concentration–response curve to TA (Fig. 3B); a pA_2 of 8.26 was calculated from these experiments.

In order to confirm the HhTAR1 sensitivity to TA and OA, other biogenic amines such as dopamine, L-DOPA, adrenaline, noradrenaline and serotonin, or important neurotransmitters such as γ-aminobutyric acid were tested at 10^{-4} mol l^{-1} as putative ligands. TA and OA were able to generate a large and robust effect as HhTAR1 agonists while the other molecules, including dopamine, elicited negligible calcium release (Fig. S3). Dopamine was able to induce a

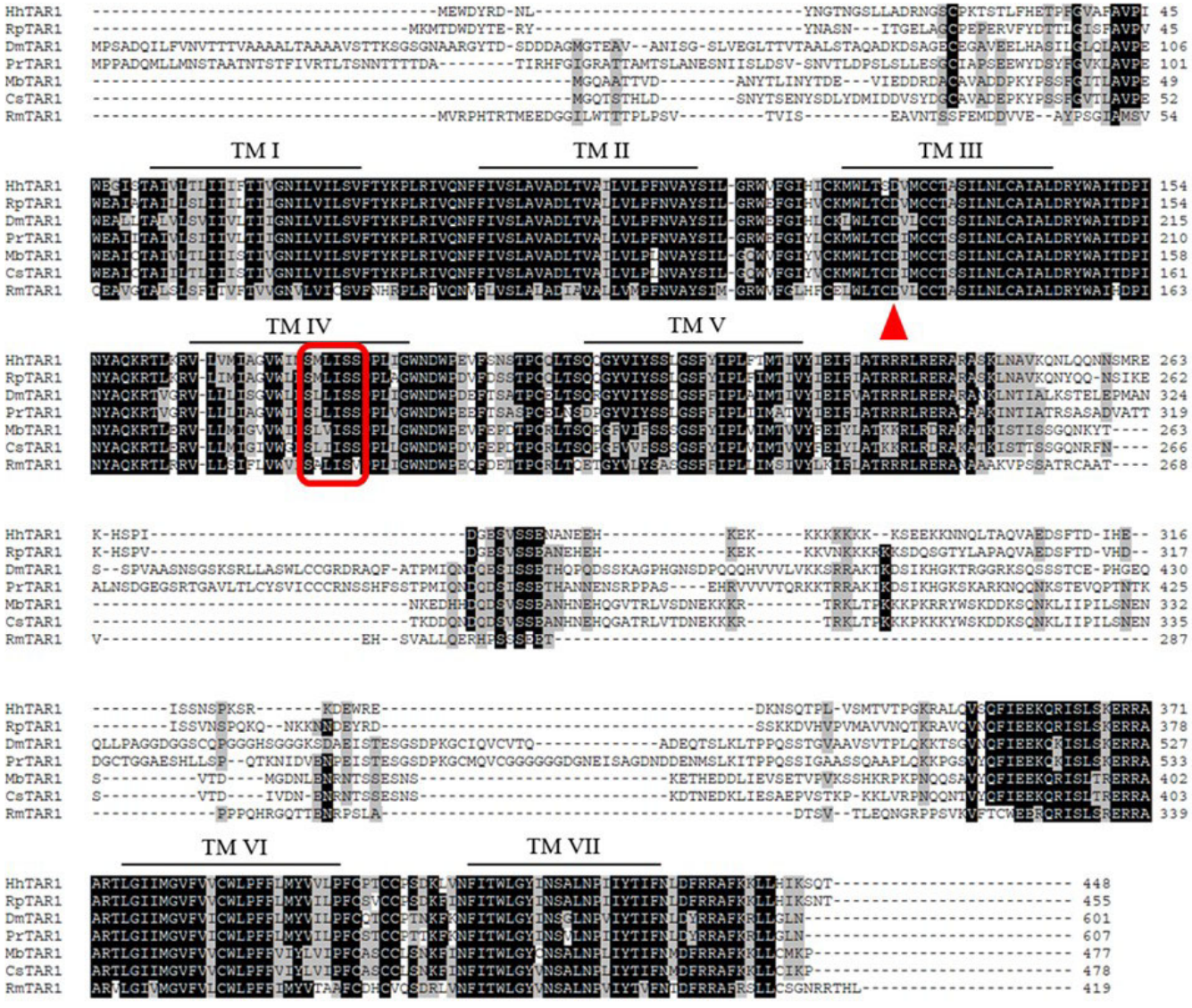

Fig. 2. Amino acid sequence alignment of HhTAR1 with orthologous receptors from *Rhodnius prolixus* (RpTAR1), *Drosophila melanogaster* (DmTAR1), *Phormia regina* (PrTAR1), *Mamestra brassicae* (MbTAR1), *Chilo suppressalis* (CsTAR1) and *Rhipicephalus microplus* (RmTAR1). The putative seven transmembrane domains (TM I–VII) are indicated by black lines. Identical residues are highlighted in black while conservative substitutions are in grey. A red triangle indicates the conserved aspartic acid D128 and the serine residues that could interact with TA are shown by a red box.

Journal of Experimental Biology (2021) 224, jeb238816. doi:10.1242/jeb.238816

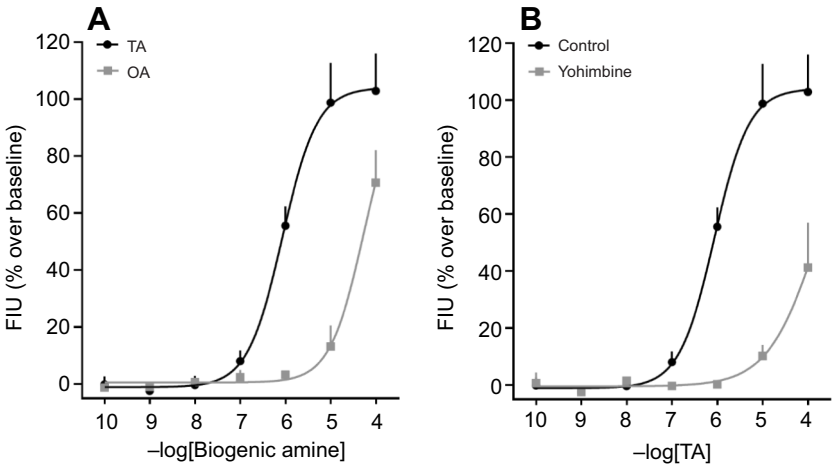

Fig. 3. Calcium mobilization assay in HhTAR1-transfected HEK293 cells. (A) Concentration–response curves to TA and octopamine (OA). FIU, fluorescence intensity units. (B) Concentration–response curves to TA in the absence (control) and presence of 1 μmol l^{-1} yohimbine, a TAR1 antagonist. Data are means±s.e.m. of three separate experiments performed in duplicate.

response when tested at 10^{-4} mol l^{-1} on *Periplaneta americana*, *Chilo suppressalis* and *R. prolixus* TAR1 (Rotte et al., 2009; Wu et al., 2014; Hana and Lange, 2017a,b). However, even in these studies, the signal was modest and it was hypothesized that the responses were probably due to the activation of endogenous dopaminergic receptors present in the cell lines used to express TAR1s.

HhTAR1 expression pattern

Given the importance of TAR1s in insect physiology and behaviour, *HhTAR1* expression profile was studied in all *H. halys* developmental stages [egg, 1st to 5th instar nymphs (L1–L5) and adult] as well as in the major organs of the adult. The analysis revealed that *HhTAR1* was mostly expressed in eggs and in 1st and 2nd instar nymphs, with a dramatic decrease in receptor mRNA levels in the later stages from

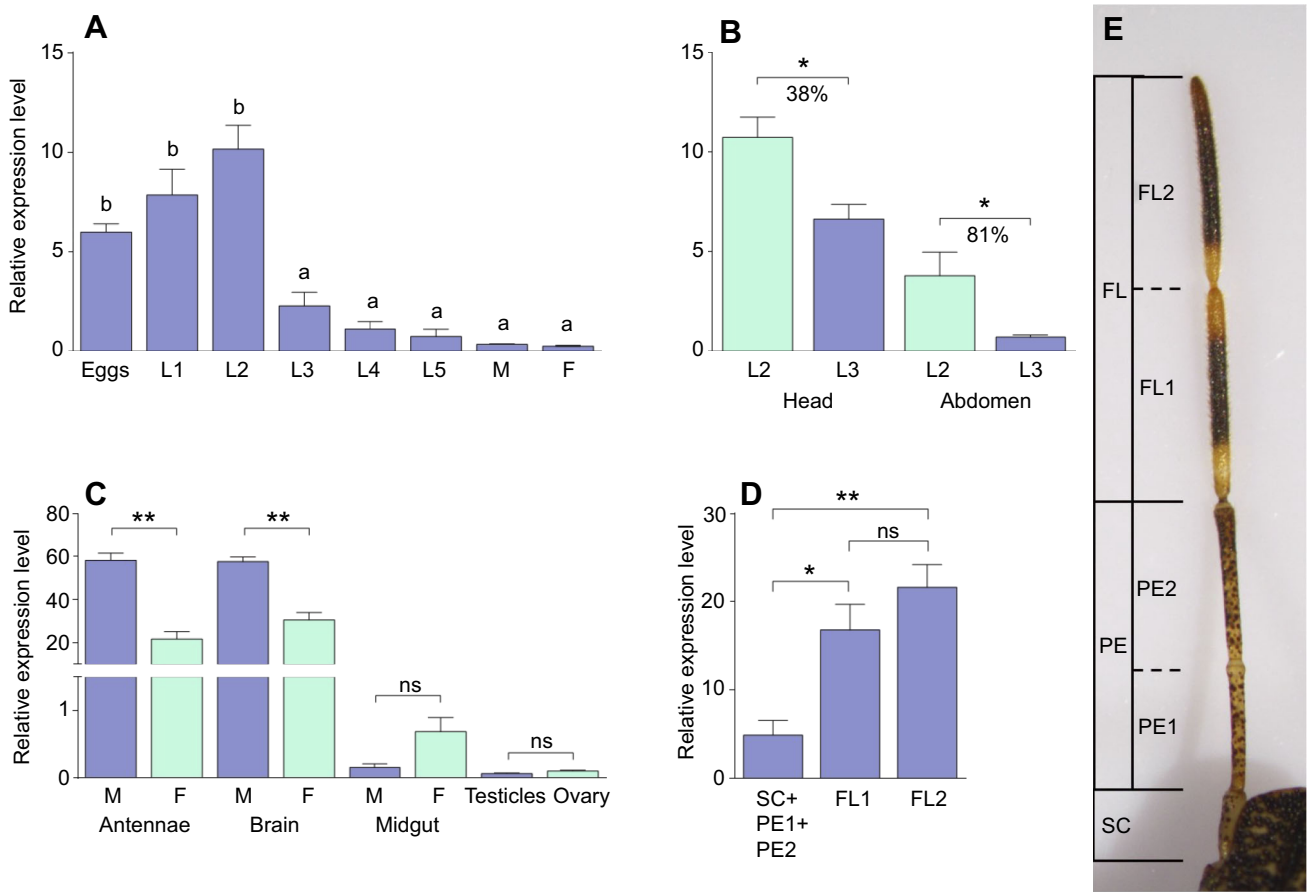

Fig. 4. mRNA expression levels of *HhTAR1* gene. (A) Expression of *HhTAR1* gene at all developmental stages: eggs, 1st to 5th instar nymphs (L1–L5), and adult males (M) and females (F). (B) Expression of *HhTAR1* in the head and abdomen of 2nd (L2) and 3rd (L3) *H. halys* instar nymphs. (C) Expression of *HhTAR1* in organs of males (M) and females (F). (D) Expression of *HhTAR1* in different parts of adult *H. halys* antennae. SC, scape; PE1, first segment of pedicel; PE2, second segment of pedicel; FL1, first segment of flagellum; FL2, second segment of flagellum. SC, PE1 and PE2 were pooled and analysed together. Data in A–D represent means±s.e.m. of at least three independent experiments performed in triplicate. **P*<0.05 and ***P*<0.01 according to one-way ANOVA followed by multiple comparisons Bonferroni *post hoc* test. (E) Antenna structure of the adult *H. halys* observed with a stereomicroscope.

the 3rd instar nymph to adult (Fig. 4A). This mRNA reduction in 2nd and 3rd instar nymphs was further investigated. The nymphs were divided in two parts: head+antennae and thorax+abdomen and the *HhTAR1* expression levels analysed. The *HhTAR1* mRNA level decrease affected both sections of 2nd and 3rd instar nymphs but to different degrees (Fig. 4B): the level in the head/antennae decreased only by 38% between L2/L3, while it dropped by 81% in the thorax/abdomen. This reveals that *HhTAR1* levels remained high in the nervous tissues while they decreased significantly in the rest of the nymph body. Among the different organs analysed (antennae, brain, midgut and gonads), the highest levels of *HhTAR1* transcript were detected in the brain and the antennae of both sexes, although they were statistically more abundant in male tissues (Fig. 4C). Furthermore, *HhTAR1* expression was investigated in all antennomeres of *H. halys*. The antenna is composed of a scape, a pedicel divided in two segments (PE1 and PE2) and a flagellum composed of two flagellomeres (FL1 and FL2) (Fig. 4E). The *HhTAR1* mRNA was detected in all antennomeres but it was 2–3 times more abundant in FL1 and FL2 in comparison to the section comprising the SC and both elements of the pedicel (Fig. 4D).

Sensilla investigation by SEM

The different expression of *HhTAR1* in antennomeres led us to further characterize the antenna. The antennae, the main organs of the olfactory system in insects, are rich in sensilla whose morphology correlates with their physiological role. We used SEM to investigate the morphology and distribution of sensilla in the different parts of adult *H. halys* antennae (Fig. 5A–I): the scape, the pedicel (PE1 and PE2) and the flagellum (flagellomeres FL1 and FL2) (Fig. 4E). In the scape and both pedicels, sporadic basiconic sensilla (Fig. 5A,B,E) were visible along with perforations classified as pit sensilla, or coeloconic sensilla, found in both pedicels (Fig. 5F,G). Several chaetic sensilla were observed in the PE2–FL1 junction area (Fig. 5C). A high number of sensilla was found in both flagellomeres, classified as trichoid (Fig. 5D,I), basiconic or grooved sensilla (Fig. 5H).

RNAi silencing of *HhTAR1* and repellency assay

A behavioural repellency assay was set up to investigate the functional role of HhTAR1 in *H. halys* behaviour and chemosensory recognition. *Halyomorpha halys* 2nd instar nymphs, the developmental stage that showed the highest *HhTAR1* expression levels, were offered a green bean in the presence or absence of the alarm pheromone component (*E*)-2-decenal and the number of individuals feeding or standing on the bean was measured during a period of 1 h (Fig. S5). As expected, (*E*)-2-decenal was able to repel approximately 50% of the nymphs compared with the acetone-treated group, used as a control (Fig. 6A). Subsequently, to assess the physiological relevance of HhTAR1 in repellency, an RNAi silencing method was applied to 2nd instar nymphs. The *HhTAR1* dsRNA was administered by topical delivery (Fig. S4) to *H. halys* 2nd instar nymphs and the silencing effect on *HhTAR1* transcript levels was evaluated by RT-qPCR 24 h after treatment. The *HhTAR1* dsRNA treatment induced a gene-silencing effect, with a 50% decrease in transcript abundance, whereas the *LacZ* dsRNA negative control did not cause any change in *HhTAR1* expression (Fig. 6B). Interestingly, the insects treated with *HhTAR1* dsRNA exhibited a reduced sensitivity to (*E*)-2-decenal, i.e. they moved towards and fed on the green bean in the presence of (*E*)-2-decenal in a similar manner to the acetone-only control (Fig. 6C). In contrast, the behaviour of nymphs treated with *LacZ* dsRNA was unmodified, and the alarm pheromone correctly repelled the insects (Fig. 6D).

DISCUSSION

Since its appearance in Europe and America, *H. halys* has caused serious damage to agriculture (Rice et al., 2014; Valentin et al., 2017). Because of its reduced susceptibility to traditional control strategies, new methods for *H. halys* containment need to be developed, identifying innovative chemical compounds as well as new targets based on the biochemistry, physiology and behaviour of this insect.

This study deals with the molecular and pharmacological characterization of the *H. halys* type 1 tyramine receptor (HhTAR1). Through RNAi silencing of *HhTAR1* it was possible to reveal the important role of HhTAR1 in physiological aspects of *H. halys*, such as the olfactory response to the alarm pheromone (*E*)-2-decenal.

The HhTAR1 polypeptide shares many structural features with TAR1s from other insects (Ohta and Ozoe, 2014). HhTAR1 contains seven highly conserved transmembrane segments, as expected for a GPCR, as well as phosphorylation and glycosylation sites, typical for this receptor class and essential for correct protein folding and receptor signalling (Nørskov-Lauritsen and Bräuner-Osborne, 2015; Alfonzo-Mèndez et al., 2017). Most of these sites (seven phosphorylation sites: T235 and S246, 260, 294, 319, 321, 364) are localized in the long intracellular loop between TM V and VI and are probably involved in receptor signalling and regulatory processes such as desensitization and internalization. Concerning the TA binding site, the main amino acid residue interacting with the endogenous agonist is an aspartic acid located in TM III and well conserved in all insect TAR1s, based on alignment studies (Braza et al., 2019). In HhTAR1, this Asp residue is found at position 128 (D128). The involvement of D128 in ligand binding was confirmed in a mutation study performed on *B. mori* TAR1 that showed that the orthologous Asp residue binds the TA amine group with an ionic bond reinforced by a H-bond (Ohta et al., 2004). The same study also showed that several serine residues in TM V stabilize the interaction between TAR1 and TA. The HhTAR1 molecular model furthermore suggests that three serine residues (found at positions 212, 213 and 216 and well conserved within TAR1 insect family) might be involved in generating the receptor binding pocket (Ohta et al., 2004; Braza et al., 2019).

The structural description encouraged us to carry out functional characterization of HhTAR1. The HhTAR1 coding region was cloned and expressed in HEK 293 cells and the recombinant receptor tested for its ability to respond to known TAR1 ligands. In the calcium mobilization assay, TA was significantly more potent than OA, as observed for other TAR1s (Gross et al., 2015; Hana and Lange, 2017a; Finetti et al., 2020). Furthermore, the effect of TA was sensitive to the antagonist yohimbine, as observed in other orthologous TAR1s (Saudou et al., 1990; Gross et al., 2015; Hana and Lange, 2017a; Finetti et al., 2020). Other biogenic amines, such as dopamine and adrenaline, were not able to activate HhTAR1 to an appreciable level, as also shown in *R. microplus* TAR1 (Gross et al., 2015) (Fig. S3).

Many studies support the physiological role of TAR1 in processes such as locomotion (Saraswati et al., 2004; Schützler et al., 2019), metabolic control (Nishimura et al., 2005; Li et al., 2017; Roeder, 2020), reproduction (Hana and Lange, 2017a,b) and olfaction (Kutsukake et al., 2000; Brigaud et al., 2009; Duportets et al., 2010; McQuillan et al., 2012; Ma et al., 2015; Zhukovskaya and Polyanovsky, 2017; Ma et al., 2019b). The *TAR1* expression patterns mirror its functional role because the *TAR1* gene is highly expressed in the CNS, salivary glands and antennae in different insect species (Duportets et al., 2010; McQuillan et al., 2012; Wu et al., 2014; El-Kholy et al., 2015; Hana and Lange, 2017a; Ma et al., 2019a;

Journal of Experimental Biology (2021) 224, jeb238816. doi:10.1242/jeb.238816

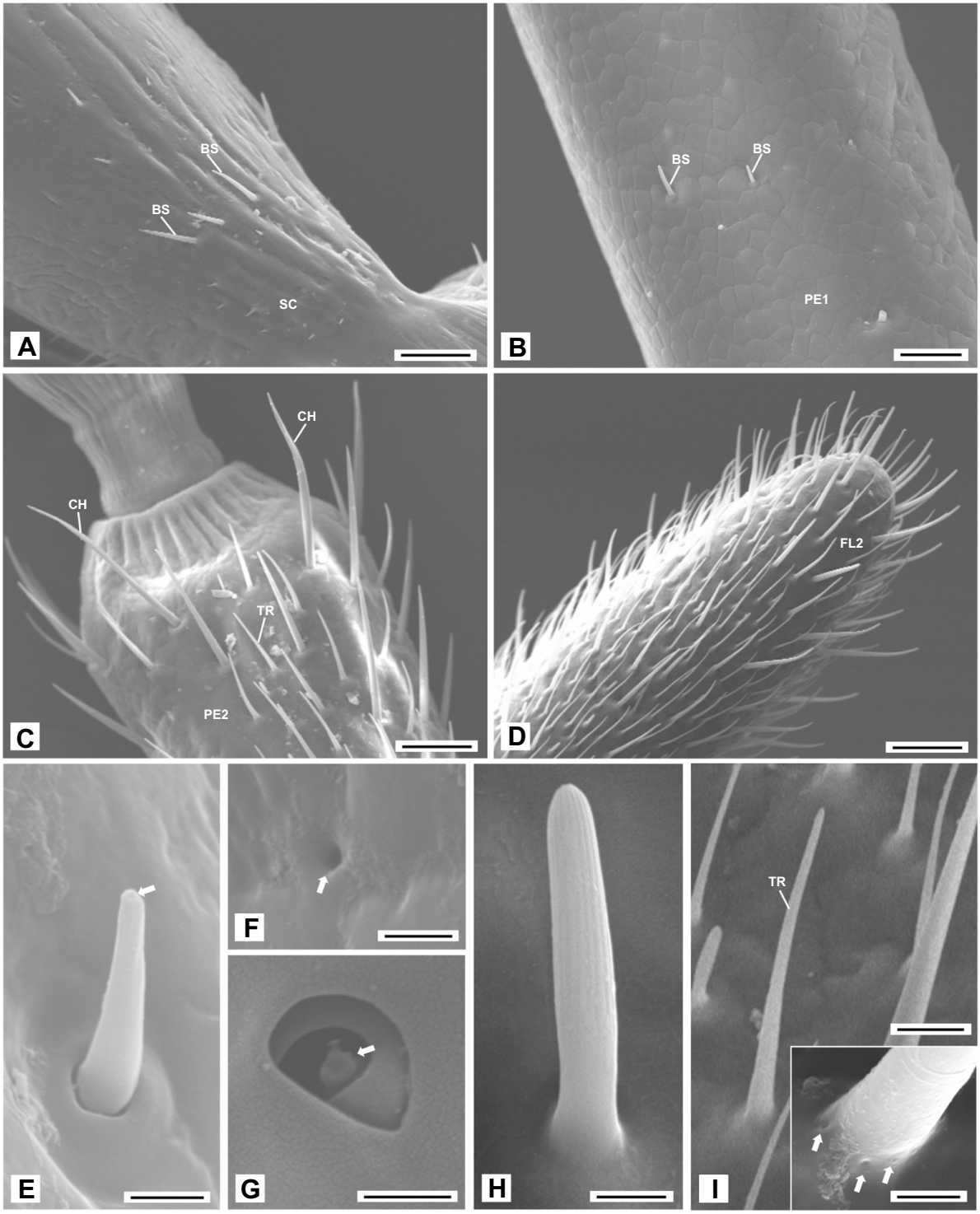

Fig. 5. Antennae of adult *H. halys* observed by scanning electron microscopy (SEM). (A) Female antenna, detail of the base of the scape. Scale bar: 50 µm. (B) Male antenna, detail of the first segment of the pedicel near the scape. Scale bar: 25 µm. (C) Male antenna, distal part of the second segment of the pedicel. Scale bar: 50 µm. (D) Male antenna, tip of the second segment of the flagellum. Scale bar: 50 µm. (E) Female antenna, basiconic sensillum of the scape with a tip perforation (arrow). Scale bar: 2.5 µm. (F) Male antenna, perforation of the pedicel (arrow). Scale bar: 1.5 µm. (G) Female antenna, pit sensillum of the pedicel, containing a peg (arrow). Scale bar: 1.5 µm. (H) Female antenna, grooved sensillum of the flagellum. Scale bar: 2.5 µm. (I) Female antenna, trichoid sensillum of the flagellum. Scale bar: 10 µm. Inset: detail of the base of the trichoid sensillum, showing microperforations (arrows). Scale bar: 2.5 µm. BS, basiconic sensillum; CH, chaetic sensillum; FL2, second segment of flagellum; GR, grooved sensillum; PE1, first segment of pedicel; PE2, second segment of pedicel; SC, scape; TR, trichoid sensillum.

Finetti et al., 2020). Two studies conducted in 2017 on the honeybee brain showed that *TAR1* was mainly expressed at the presynaptic sites in antennal lobe OSNs and in the mushroom body PNs, which are essential structures for the olfactory system in insects (Sinakevitch et al., 2017; Thamm et al., 2017). Similarly, in *H. halys*, *HhTAR1* appeared strongly expressed in brain and antennae but was less

Journal of Experimental Biology (2021) 224, jeb238816. doi:10.1242/jeb.238816

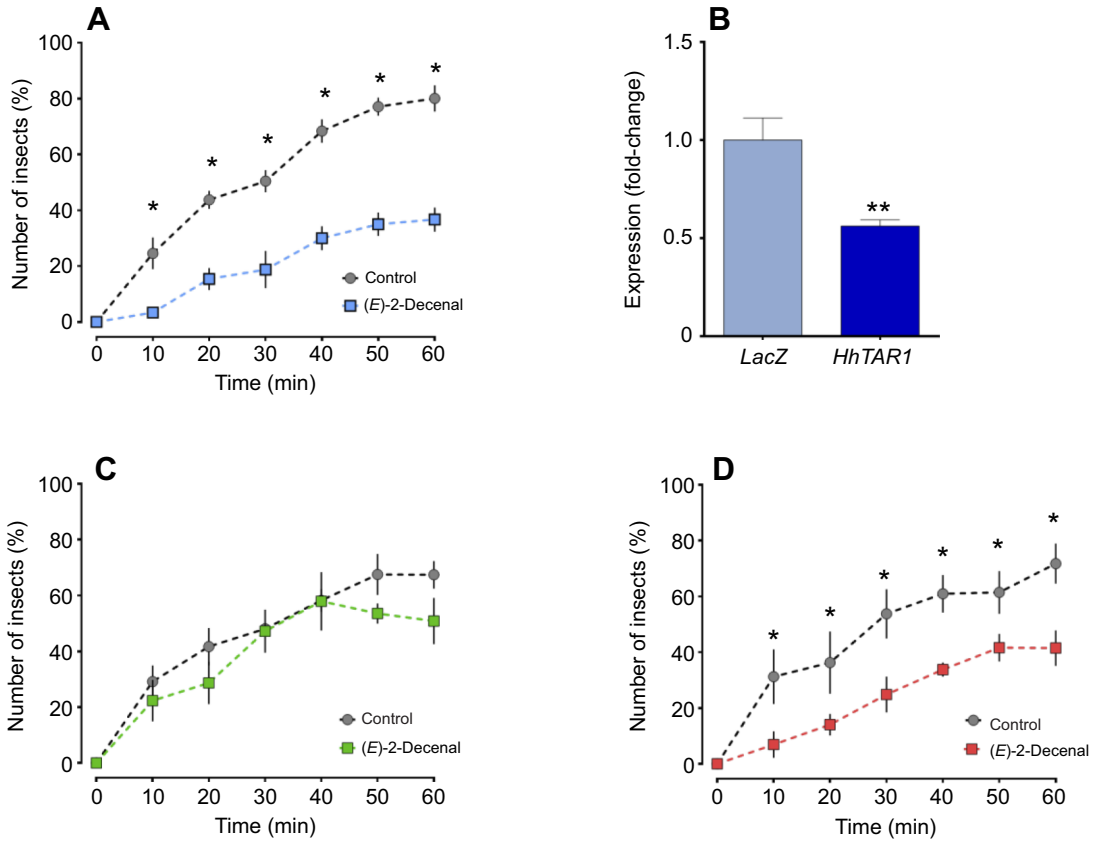

Fig. 6. Olfactory modulation of *H. halys* 2nd instar nymphs. (A) Behavioural repellency assay on 2nd instar *H. halys* nymphs in the presence or absence (control) of the alarm pheromone (*E*)-2-decenal. (B) Reduction in *HhTAR1* transcript levels by RNAi. Each bar shows the mean fold-change (±s.e.m.) of four independent replicates of *H. halys* 2nd instar nymphs 24 h after gene-specific dsRNA treatment, topically delivered. *LacZ* dsRNA treatment was used as a negative control. ***P*<0.01 versus control according to Student's *t*-test. (C,D) Behaviour assay after (C) *HhTAR1* dsRNA or (D) *LacZ* dsRNA administration in the presence or absence of (*E*)-2-decenal. Data are means±s.e.m. of four independent replicates for a total of at least 50 insects tested. **P*<0.05 versus control according to two-way ANOVA (time×treatment) followed by Dunnett's *post hoc* test.

strongly expressed in the midgut and reproductive systems of adults. Furthermore, *HhTAR1* mRNA was more abundant in the male brain than in the female one. This sex-dependent *TAR1* expression was also detected in *D. suzukii* (Finetti et al., 2020) and *Plutella xylostella* (Ma et al., 2019a), suggesting that TAR1 could be involved in male-specific functions such as development as well as reproduction. The high brain expression of *HhTAR1* correlates well with the abundance of TAR1 in the CNS of numerous insect species (El-Kholy et al., 2015; Hana and Lange, 2017a; Finetti et al., 2020), where it regulates several sensory processes (Roeder et al., 2003; Lange, 2009; Ohta and Ozoe, 2014; Neckameyer and Leal, 2017). Interestingly, *HhTAR1* was also highly abundant in the antennae. Actually, several studies have shown that TAR1 is expressed in antennae although its role in these structures is still unclear. A possible correlation between TAR1 and olfaction was established for the first time in 2000 (Kutsukake et al., 2000). This study characterized a *D. melanogaster* TAR1-mutant line, called *honoka*, whose behavioural responses to repellents were reduced in comparison to those of wild-type flies. Our data also revealed that *HhTAR1* is more expressed in the male antennae of *H. halys* than in female antennae. These results suggest that TAR1, besides being associated with olfactory repellence processes, could also play a role in responses to olfactory reproductive stimuli, such as pheromones, or in mating behaviours (Mazzoni et al., 2017). The *HhTAR1* mRNA was more abundant in the two flagellomeres FL1 and FL2 with a 6-fold difference in comparison to levels in the other antennal structures. A typical insect antenna contains numerous sensilla, essential structures for smell, taste, mechanoreception and thermo-hygroperception (Zacharuk, 1985). The great number of sensilla in the apical parts of the *H. halys* antennae correlates with the high *HhTAR1* expression level in the same areas, further strengthening a role for TAR1 in olfaction. As the physiological role of each sensilla may be predicted based on their morphology, size and distribution (Keil, 1999), the *H. halys* sensilla was investigated by SEM. Different types of sensilla have been classified in the Pentatomidae, including basiconic, trichoid, coeloconic and chaetic sensilla (Brèzot et al., 1997). The most abundant structures in FL1 and FL2 segments of the adult *H. halys* were the trichoid sensilla followed by basiconic sensilla and grooved sensilla as also observed by Ibrahim et al. (2019) in the same insect. The trichoid sensilla and basiconic sensilla share olfactory functions (Toyama et al., 2006), as suggested by the presence on the surface of distinctive microperforations necessary to connect the odour molecules with the olfactory receptors in the OSNs (Zacharuk, 1985). It is difficult to associate each type of sensillum with a specific olfactory-mediated behaviour, but the removal of both FLs completely inhibited adult *H. halys* aggregation, indicating that these structures, and probably also the trichoid sensilla and basiconic sensilla are necessary to perceive the aggregation pheromone (Toyama et al., 2006). However, sporadic basiconic sensilla have been observed in the scape and both segments of the pedicel (PE1 and PE2) along with structures identified as pit sensilla or coeloconic sensilla that could be involved in thermo-hygroperception (Altner and Prillinger, 1980). It is

interesting to note that *HhTAR1* is more highly expressed in the flagellum than in the scape and pedicel, suggesting a correlation between TAR1 and olfactory sensilla. These data would therefore suggest an important role for HhTAR1 in olfactory processes. Interestingly, *HhTAR1* also showed high expression levels in eggs and in 1st and 2nd instar nymphs, followed by a dramatic decrease from the 3rd instar nymphs onwards. The high *TAR1* expression level in eggs has also been observed in *P. xylostella* (Ma et al., 2019a,b). However, information about the role of TA and TAR1 in embryogenesis is limited for *D. melanogaster*, in which the *TAR1* gene exhibits a dynamic expression pattern during embryo maturation inside the eggs, with a peak corresponding to nervous tissue formation (Hannon and Hall, 1996). In their study, the authors hypothesized that the decline in TAR1 expression in larval stages may be explained by the relative decrease in the ratio of neuronal versus non-neuronal tissue. The results also revealed that between 2nd and 3rd instar nymphs, *HhTAR1* expression decreased more (about 80%) in the abdomen and thorax tissues in comparison to the head. A similar result was observed also in adults, where *HhTAR1* levels remained high in brain and antennae in comparison to other tissues. Previous studies observed that *H. halys* nymphs exhibited 4 times higher mortality than adults after treatment with essential oils for 1 or 48 h (Bergmann and Raupp, 2014). The high *HhTAR1* expression in the CNS and antennae of nymphs could explain the greater sensitivity to volatile compounds with insecticide properties, such as essential oils. It is known that TAR1 is a putative target for biopesticides, such as monoterpenes (Gross et al., 2017; Finetti et al., 2020). Although their toxicity in vertebrates has not been ascertained, monoterpenes are currently used as repellents against insect pests (Reis et al., 2016).

The analysis of *HhTAR1* expression patterns together with the SEM observations on *H. halys* antennae strongly suggest a connection between HhTAR1 and *H. halys* olfactory regulation. To better investigate this aspect, *HhTAR1* was silenced by RNAi in young nymphs. In recent years, several Hemiptera genes have been successfully silenced through this method (Christiaens and Smagghe, 2014; Bansal et al., 2016; Ghosh et al., 2017; Lu et al., 2017; Mogilicherla et al., 2018; Riga et al., 2019). In these studies, RNAi silencing was successfully performed on *H. halys* using microinjection and feeding as delivery methods. A 1 µg sample of dsRNA injected into *H. halys* adults was able to silence several target genes by 60–80% after 72 h (Mogilicherla et al., 2018). In contrast, when the dsRNA solution was delivered by feeding to *H. halys* 2nd and 4th instar nymphs, some target genes were silenced only by 40–80% (Ghosh et al., 2017). In these two studies (Mogilicherla et al., 2018 and Ghosh et al., 2017), the dsRNA was delivered exclusively by microinjection or by feeding but both these delivery methods are problematic. Microinjection requires experience and specific instruments to control the injected volume, as well as minimizing the wound, which often causes a drastic increasing in mortality (Christiaens et al., 2020). However, through microinjection of *HhTAR1* RNAi we were able to obtain a downregulation in *H. halys* 2nd instar nymphs (data not shown) but with an extremely high mortality level. dsRNA delivery by feeding requires a large amount of dsRNA and it does not allow control of the amount of dsRNA ingested by each insect (Joga et al., 2016). dsRNA topical delivery has recently been tested in two Hemiptera species, *Diaphorina citri* and *Acyrthosiphon pisum*. In *D. citri*, 20 ng of dsRNA solution topically delivered on the abdomen was able to silence several *Cyp* genes by about 70–90% (Killiny et al., 2014). In *A. pisum*, 120 ng of dsRNA solution induced a downregulation of the target gene by 90% after 24–36 h (Niu et al., 2019). Accordingly, in *H. halys* 2nd instar nymphs (rich in *HhTAR1* mRNA), a 100 ng dose of *HhTAR1* dsRNA topically delivered appeared sufficient to silence *HhTAR1* by about 50% after 24 h, as verified by RT-qPCR. The different RNAi efficiency observed between *D. citri*, *A. pisum* and *H. halys* could be based on the different body structure: the abdominal cuticle of *H. halys* nymphs is thicker than that of *D. citri* and *A. pisum*, an aspect that could limit absorption of dsRNA solution. Regardless, this is the first time that RNAi-mediated gene silencing has been induced by topical delivery in *H. halys*. Although topically delivered dsRNA is less efficient as a gene silencer in *H. halys*, the administered amount of dsRNA is lower than that for microinjection and the feeding applications. Reducing the amount of dsRNA could be an effective strategy to prevent off-target effects (Romeis and Widmer, 2020).

Following *HhTAR1* silencing, olfactive performance of *H. halys* 2nd instar nymphs was tested by an innovative behavioural assay. This assay measured the repellent effect of (*E*)-2-decenal, one of the main alarm compounds released by *H. halys* under threat, on 2nd instar nymphs (Zhong et al., 2017, 2018; Nixon et al., 2018). The *HhTAR1* dsRNA treatment caused a reduced sensitivity to (*E*)-2-decenal in comparison to the *LacZ* dsRNA control nymphs, suggesting that the (*E*)-2-decenal-mediated alarm requires a functional TAR1. Based on the *HhTAR1* expression pattern, it is possible that RNAi-mediated downregulation of the receptor might affect both the brain and antennae of *H. halys*, the regions showing the highest receptor expression. Sinakevitch et al. (2017) observed that *A. mellifera* TAR1 was expressed in the presynaptic regions of the ORN axons that innervate the antennal lobe glomeruli and that could control the transduction signal through TA. Based on this study it might be that, after *HhTAR1* RNAi treatment, the presynaptic regions of the ORN axons could also have a lower abundance of *TAR1* in *H. halys* and, accordingly, show an impairment in the transmission of the pheromone-stimulated signal.

However, in a study performed on *Manduca sexta*, the injection of TA directly into the sensillum modulated the response to sexual pheromones. The authors advanced the hypothesis that TA, through TAR binding, regulated the levels of both Ca^{2+} and cAMP, which in turn regulated the olfactory receptor sensitivity to pheromones (Flecke and Stengl, 2009). Therefore, the downregulation of *HhTAR1* could affect the intracellular cascade involving Ca^{2+} and cAMP content triggered by the pheromone-mediated olfactory receptor activation.

As *H. halys* is a relatively new research target and many tools available for model species cannot be applied to this species, we cannot reasonably attribute the reduced sensitivity to the alarm pheromone (*E*)-2-decenal to the neural or the antennal regions. Further investigation will be needed to understand whether the RNAi-mediated *TAR1* downregulation affects the complex pheromone olfactory perception in a peripheral or central way.

In conclusion, HhTAR1 could play a relevant role in the *H. halys* olfactory network, contributing to the modulation of olfaction-mediated behaviours, such as the reception of alarm pheromone compounds. A more detailed characterization of the interconnections between TAR1 and the olfactory system will open the way for developing TAR1-targeting volatile compounds, such as essential oils, with both repellent and insecticidal properties against *H. halys*.

Acknowledgements

The authors would like to thank Dr Santolo Francati (University of Bologna) for providing *H. halys* adults, Dr Morena De Bastiani (University of Ferrara) for technical assistance, Prof. Stefano Della Longa (University of L'Aquila) and Prof. Alessandro Arcovito (Università Cattolica del Sacro Cuore, Rome) for molecular modelling advice, Dr Federica Albanese (University of Ferrara) and Dr Milvia Chicca (University of Ferrara) for language revision.

Competing interests
The authors declare no competing or financial interests.

Author contributions
Conceptualization: G.C., G.B.; Methodology: L.F., M.P., S.C.; Software: L.F.; Validation: L.F.; Formal analysis: L.F., S.C.; Investigation: L.F., M.P.; Data curation: L.F., M.P.; Writing - original draft: L.F.; Writing - review & editing: G.C., C.S., G.B.; Supervision: G.B.; Project administration: G.B.; Funding acquisition: G.C., G.B.

Funding
This study was funded by Camera di Commercio Industria, Artigianato e Agricoltura of Ferrara Bando 2018 and by the Emilia Romagna Region within the Rural Development Plan 2014-2020 Op. 16.1.01 – GO EIP-Agri - FA 4B, Pr. 'ALIEN.STOP', coordinated by CRPV.

References

Alfonzo-Mèndez, M. A., Alcàntara-Hernàndez, R. and Garcìa-Sàinz, J. A. (2017). Novel structural approaches to study GPCR regulation. *Int. J. Mol. Sci.* **18**, 27. doi:10.3390/ijms18010027

Altner, H. and Prillinger, L. (1980). Ultrastructure of invertebrate chemo, thermo, and hygroreceptors and its functional significance. *Int. Rev. Cytol.* **67**, 69-139. doi:10.1016/S0074-7696(08)62427-4

Amin, H. and Lin, C. A. (2019). Neuronal mechanisms underlying innate and learned olfactory processing in *Drosophila*. *Curr. Opin. Insect Sci.* **36**, 9-17. doi:10.1016/j.cois.2019.06.003

Bansal, R., Mittaperry, P., Chen, Y., Mamidal, P., Zhao, C. and Michel, A. (2016). Quantitative RT-PCR gene evaluation and RNA interference in the Brown Marmorated Stink Bug. *PLos ONE* **11**, e0152730. doi:10.1371/journal.pone.0152730

Bayliss, A., Roselli, G. and Evans, P. D. (2013). A comparison of the signalling properties of two tyramine receptor from Drosophila. *J. Neurochem.*. **125**, 37-48. doi:10.1111/jnc.12158

Bergmann, E. and Raupp, M. (2014). Efficacies of common ready to use insecticides against *Halyomorpha halys* (Hemipter: Pentatomidae). *Fla. Entomol.* **97**, 791-800. doi:10.1653/024.097.0262

Blenau, W. and Baumann, A. (2003). Aminergic signal transduction in invertebrates: focus on tyramine and octopamine receptors. *Recent Res. Dev. Neurochem.* **6**, 225-240.

Blenau, W., Balfanz, S. and Baumann, A. (2000). Amtyr1: Characterization of a gene from honeybee (*Apis mellifera*) brain encoding a functional tyramine receptor. *J. Neurochem.* **74**, 900-908. doi:10.1046/j.1471-4159.2000.0740900.x

Braza, M. K. E., Gazmen, J. D. N., Yu, E. T. and Nellas, R. B. (2019). Ligand-induced conformational dynamics of a tyramine receptor from *Sitophilus oryzae*. *Sci. Rep.* **9**, 16275. doi:10.1038/s41598-019-52478-x

Brèzot, P., Taudan, D. and Renon, M. (1997). Sense organs on the antennal flagellum of the green stink bug, *Nezara viridula* (L.) (Heteroptera: Pentatomidae): sensillum types and numerical growth during the post-embryonic development. *Int. J. Insect Morphol. Embryol.* **25**, 427-441. doi:10.1016/S0020-7322(96)00012-8

Brigaud, L., Grosmaître, X., François, M. C. and Jacqion-Joly, E. (2009). Cloning and expression pattern of a putative octopamine/tyramine receptor in antennae of the noctuid moth *Mamestra brassicae*. *Cell Tissue Res.* **335**, 445-463. doi:10.1007/s00441-008-0722-5

Carey, A. F. and Carlson, J. R. (2011). Insect olfaction from model systems to disease control. *Proc. Natl Acad. Sci. USA* **108**, 12987-12995. doi:10.1073/pnas.1103472108

Caron, S. J. C., Ruta, V., Abbott, L. F. and Axel, R. (2013). Random convergence of olfactory inputs in the *Drosophila* mushroom body. *Nature* **497**, 113-117. doi:10.1038/nature12063

Cesari, M., Maistrello, L., Piemontese, L., Bonini, R., Dioli, P., Lee, W., Park, C.-G., Partsinevelos, G. K., Rebecchi, L. and Guidetti, R. (2018). Genetic diversity of the Brown Marmorated Stink Bug *Halyomorpha halys* in the invaded territories of Europe and its patterns of diffusion in Italy. *Biol. Invasions* **20**, 1073-1092. doi:10.1007/s10530-017-1611-1

Chenn, V. B., Arendall, W. B., Headd, J. J., Keedy, D. A., Immormino, R. M., Kapral, G. J., Murray, L. W., Richardson, J. S. and Richardson, D. C. (2010). *Acta Crystallographica* **66**, 16-21. doi:10.1107/S0907444909042073

Christiaens, O. and Smagghe, G. (2014). The challenge of RNAi-mediated control of hemipterans. *Curr. Opin. Insect Sci.* **6**, 15-21. doi:10.1016/j.cois.2014.09.012

Christiaens, O., Whyard, S., Vèlez, A. M. and Smagghe, G. (2020). Double-stranded RNA technology to control insect pest: current status and challenges. *Front. Plant Sci.* **11**: 451. doi:10.3389/fpls.2020.00451

Duportets, L., Barrozo, R. B., Bozzolan, F., Gaertner, C., Anton, S., Gadenne, C. and Debernard, S. (2010). Cloning of an octopamine/tyramine receptor and plasticity of its expression as a function of adult sexual maturation in the male moth *Agrotis ipsilon*. *Insect Mol. Biol.* **19**, 489-499. doi:10.1111/j.1365-2583.2010.01009.x

El-Kholy, S., Stephano, F., Li, Y., Bhandari, A., Fink, C. and Roeder, T. (2015). Expression analysis of octopamine and tyramine receptors in Drosophila. *Cell Tissue Res.* **361**, 669-684. doi:10.1007/s00441-015-2137-4

Enan, E. E. (2005). Molecular response of *Drosophila melanogaster* tyramine receptor cascade to plant essential oils. *Insect Biochem. Mol. Biol.* **35**, 309-321. doi:10.1016/j.ibmb.2004.12.007

Finetti, L., Ferrari, F., Cassaneli, S., De Bastiani, M., Civolani, S. and Bernacchia, G. (2020). Modulation of *Drosophila suzukii* type 1 tyramine receptor (DsTAR1) by monoterpenes: a potential new target for next generation biopesticides. *Pestic. Biochem. Physiol.* **165**, 104549. doi:10.1016/j.pestbp.2020.02.015

Flecke, C. and Stengl, M. (2009). Octopamine and tyramine modulate pheromone-sensitive olfactory sensilla of the hawkmonth *Manduxa sexta* in time-dependent manner. *J. Comp. Physiol. A* **195**, 529-545. doi:10.1007/s00359-009-0429-4

Gadenne, C., Barrozo, R. B. and Anton, S. (2016). Plasticity in insect olfaction: to smell or not to smell? *Annu. Rev. Entomol.* **61**, 317-333. doi:10.1146/annurev-ento-010715-023523

Ghosh, S. K. B., Hunter, W. B., Park, A. L. and Gundersen-Rindal, D. E. (2017). Double strand RNA delivery system for plant-sap-feeding insects. *PLoS ONE* **12**, e0171861. doi:10.1371/journal.pone.0171861

Gross, A. D., Temeyer, K. B., Day, T. A., Pérez de Leòn, A. A., Kimber, M. J. and Coats, J. R. (2015). Pharmacological characterization of a tyramine receptor from the southern cattle tick, *Rhipicephalus* (*Boophilus*) *microplus*. *Insect Biochem. Mol. Biol.* **63**, 47-53. doi:10.1016/j.ibmb.2015.04.008

Gross, A. D., Temeyer, K. B., Day, T. A., Pérez de León, A. A., Kimber, M. J. and Coats, J. R. (2017). Interaction of plant essential oil terpenoids with the southern cattle tick tyramine receptor: A potential biopesticide target. *Chem-Biol. Interact.* **263**, 1-6. doi:10.1016/j.cbi.2016.12.009

Hana, S. and Lange, A. B. (2017a). Cloning and functional characterization of Octβ2-receptor and Tyr1-receptor in the chagas disease vector, *Rhodnius prolixus*. *Front. Physiol.* **8**, 744. doi:10.3389/fphys.2017.00744

Hana, S. and Lange, A. B. (2017b). Octopamine and tyramine regulate the activity of reproductive visceral muscles in the adult female blood-feeding bug, *Rhodnius prolixus*. *J. Exp. Biol.* **220**, 1830-1836. doi:10.1242/jeb.156307

Hannon, F. and Hall, L. M. (1996). Temporal and spatial expression patterns of two G-protein coupled receptors in *Drosophila melanogaster*. *Invertebr. Neurosci.* **2**, 71-83. doi:10.1007/BF02336662

Haye, T., Gariepy, T. D., Hoelmer, K., Rossi, J.-P., Streito, J. C., Tassus, T. and Desneux, N. (2015). Range expansion of the invasive Brown Marmorated Stink Bug, *Halyomorpha halys*: an increasing threat to field, fruit and vegetable crops worldwide. *J. Pest Sci.* **88**, 665-673. doi:10.1007/s10340-015-0670-2

Hoebeke, E. R. and Carter, M. E. (2003). *Halyomorpha halys* (Stål) (Heteroptera: Pentatomidae): A polyphagous plant pest from Asia newly detected in North America. *Proc. Entomol. Soc. Washington* 105, 225-237.

Ibrahim, A., Giovannini, I., Anfora, G., Rossi Stacconi, M. V., Malek, R., Maistrello, L., Guidetti, R. and Romani, R. (2019). A closer look at the antennae of the invasive *Halyomorpha halys*: fine structure of the sensilla. *Bull. Insectol.* **72**, 187-199.

Jefferis, G. S. X. E., Potter, C. J., Chan, A. M., Marin, E. C., Rohlfing, T., Maurer, C. R. and Luo, L. (2007). Comprehensive maps of *Drosophila* higher olfactory centers: spatially segregated fruit and pheromone representation. *Cell* **128**, 1187-1203. doi:10.1016/j.cell.2007.01.040

Joga, M. R., Zotti, M. J., Smagghe, G. and Christiaens, O. (2016). RNAi efficiency, systemic properties, and novel delivery methods for pest insect control: what we know so far. *Front. Physiol.* **7**, 553. doi:10.3389/fphys.2016.00553

Keil, T. A. (1999). Morphology and development of the peripheral olfactory organs. In *Insect Olfaction* (ed. B. S. Hansson), pp. 5-47. Berlin, Germany: Springer.

Kenakin, T. A. (2014). *A Pharmacology Primer. Techniques for More Effective and Strategic Drug Discovery*, 4th Edition. Elsevier Science Publishing.

Killiny, N., Hajeri, S., Tiwari, S., Gowda, S. and Stelinski, L. L. (2014). Double-stranded RNA uptake through topical application, mediates silencing of five CYP4 genes and suppresses insecticide resistance in *Diaphorina citri*. *PLoS ONE* **9**, e110536. doi:10.1371/journal.pone.0110536

Kumar, R. (2019). Molecular markers and their application in the monitoring of acaricide resistance in Rhipicephalus microplus. *Exp. Appl. Acarol* **78**, 149-172. doi:10.1007/s10493-019-00394-0

Kutsukake, M., Komatsu, A., Yamamoto, D. and Ishiwa-Chigusa, S. (2000). A tyramine receptor gene mutation causes a defective olfactory behaviour in *Drosophila melanogaster*. *Gene* **245**, 31-42. doi:10.1016/S0378-1119(99)00569-7

Kyte, A. and Doolittle, F. R. (1982). A simple method for displaying the hydropathic character of a protein. *J. Mol. Biol.* **157**, 105-132. doi:10.1016/0022-2836(82)90515-0

Lange, A. B. (2009). Tyramine: from octopamine precursor to neuroactive chemical in insects. *Gen. Comp. Endocrinol.* **162**, 18-26. doi:10.1016/j.ygcen.2008.05.021

Larionov, A., Krause, A. and Miller, W. (2005). A standard curve-based method for relative real time PCR data processing. *BMC Bioinformatics* **6**, 62. doi:10.1186/1471-2105-6-62

Le Corre, P., Parmer, R. J., Kailasam, M. T., Kennedy, B. P., Skaar, T. P., Ho, H., Leverge, R., Smith, D. W., Ziegler, M. G., Insel, P. A. et al. (2004). Human

sympathetic activation by alpha2-adrenergic blockade with yohimbine: Biomodal, epistatic influence of cytochrome P450-mediated drug metabolism. *Clin. Pharmacol. Ther.* **76**, 139-153. doi:10.1016/j.clpt.2004.04.010

Lee, D.-H., Short, B. D., Joseph, S. V., Bergh, J. C. and Leskey, T. C. (2013). Review of the biology, ecology and management of *Halyomorpha halys* (Hemiptera: Pentatomidae) in China, Japan, and the Republic of Korea. *Environ. Entomol.* **42**, 627-641. doi:10.1603/EN13006

Leskey, T. C. and Nielsen, A. L. (2018). Impact of the Brown Marmorated Stink Bug in North America and Europe: history, biology, ecology and management. *Annu. Rev. Entomol.* **63**, 599-608. doi:10.1146/annurev-ento-020117-043226

Li, Y., Tiedemann, L., Von Frieling, J., Nolte, S., El-Kholy, S., Stephano, F., Gelhaus, C., Bruchhaus, I., Fink, C. and Roeder, T. (2017). The role of monoaminergic neurotransmission for metabolic control in the fruit fly *Drosophila melanogaster*. *Front. Syst. Neurosci.* **11**, 60. doi:10.3389/fnsys.2017.00060

Lu, Y., Chen, M., Reding, K. and Pick, L. (2017). Establishment of molecular genetic approaches to study gene expression and function in an invasive hemipteran, *Halyomorpha halys*. *EvoDevo* **8**, 15. doi:10.1186/s13227-017-0078-6

Ma, Z., Guo, X., Lei, H., Li, T., Hao, S. and Kang, L. (2015). Octopamine and tyramine respectively regulate attractive and repulsive behavior in locust phase changes. *Sci. Rep.* **5**, 8036. doi:10.1038/srep08036

Ma, H., Huang, Q., Lai, X., Liu, J., Zhu, H., Zhou, Y., Deng, X. and Zhou, X. (2019a). Pharmacological properties of the type 1 tyramine receptor in the Diamondback moth, *Plutella xylostella*. *Int. J. Mol. Sci.* **20**, 2953. doi:10.3390/ijms20122953

Ma, Z., Guo, X. and Liu, J. (2019b). Traslocator protein mediates olfactory repulsion. *FASEB J.* **34**, 513-524. doi:10.1096/fj.201900528RR

Mazzoni, V., Polajnar, J., Baldini, M., Stacconi, M. V. R., Anfora, G., Guidetti, R. and Maistrello, L. (2017). Use of substrte-borne vibrational signals to attact the brown marmorated stink bug, *Halyomorpha halys*. *J. Pest Sci.* **90**, 1219-1229. doi:10.1007/s10340-017-0862-z

McQuillan, H. J., Barron, A. B. and Mercer, A. R. (2012). Age- and behaviour-related changes in the expression of biogenic amine receptor genes in the antennae of honeybees (*Apis mellifera*). *J. Comp. Physiol. A* **198**, 753-761. doi:10.1007/s00359-012-0745-y

Mogilicherla, K., Howell, J. L. and Palli, S. R. (2018). Improving RNAi in the bron marmorated stink bug: identification of target genes and reference genes for RT-qPCR. *Sci. Rep.* **8**:3720. doi:10.1038/s41598-018-22035-z

Mustard, J. A., Kurshan, P. T., Hamilton, I. S., Blenau, W. and Mercer, A. R. (2005). Developmental expression of a tyramine receptor gene in the brain of the honeybee, *Apis mellifera*. *J. Comp. Neurol.* **483**, 66-75. doi:10.1002/cne.20420

Neckameyer, W. S. and Leal, S. M. (2017). Diverse functions of insect biogenic amines as neurotransmitters, neuromodulators and neurohormones. In. *Hormones, Brain and Behavior*, 3rd edn, pp. 368-400. Oxford: Academic Press.

Nielsen, A. L., Chen, S. F. and Fleischer, S. J. (2016). Coupling, developmental, physiology, photoperiod and temperature to model phenology and dynamics of an invasive Heteropteran, *Halyomorpha halys*. *Front. Physiol.* **7**,165. doi:10.3389/fphys.2016.00165

Nishimura, T., Seto, A., Nakamura, K., Miyama, M., Nagao, T., Tamotsu, S., Yamaoka, R. and Ozaki, M. (2005). Experiental effects of appetitive and nonappetitive odors on feeding behavior in the blowfly, *Phormia regina*: a putative role for tyramine in appetite regulation. *J. Neurosci.* **25**, 7507-7516. doi:10.1523/JNEUROSCI.1862-05.2005

Niu, J., Yang, W.-J., Tian, Y., Fan, J.-Y., Ye, C., Shang, F., Ding, B.-Y., Zhang, J., An, X., Yang, L. et al. (2019). Topical dsRNA delivery induces gene silencing and mortality in the pea aphid. *Pest Manag. Sci.* **75**, 2873-2881. doi:10.1002/ps.5457

Nixon, L. J., Morrison, W. R., Rice, K. B., Brockerhoff, E. G., Leskey, T. C., Guzman, F., Khrimian, A., Goldson, S. and Rostàs, M. (2018). Identification of volatiles released by diapausing brown marmorated stink bug, *Halyomorpha halys* (Hemiptera: Pentatomidae). *PLoS ONE* **13**, e0191223. doi:10.1371/journal.pone.0191223

Nørskov-Lauritsen, L. and Bräuner-Osborne, H. (2015). Role of post-translational modifications on structure, function and pharmacology of class C G protein-coupled receptors. *Eur. J. Pharmacol.* **763**, 233-240. doi:10.1016/j.ejphar.2015.05.015

Ohta, H. and Ozoe, Y. (2014). Molecular signalling, pharmacology, and physiology of octopamine and tyramine receptors as potential insect pest control targets. *Adv. Insect Physiol.* **46**, chapter two. doi:10.1016/B978-0-12-417010-0.00002-1

Ohta, H., Utsumi, T. and Ozoe, Y. (2003). B96Bom encodes a *Bombyx mori* tyramine receptor negatively coupled to adenylate cyclase. *Insect Mol. Biol.* **12**, 217-223. doi:10.1046/j.1365-2583.2003.00404.x

Ohta, H., Utsumi, T. and Ozoe, Y. (2004). Amino acid residues involved in interaction with tyramine in the *Bombyx mori* tyramine receptor. *Insect Mol. Biol.* **13**, 531-538. doi:10.1111/j.0962-1075.2004.00511.x

Pauls, D., Blechschmidt, C., Frantzmann, F., Jundi, B. and Selcho, M. (2018). A comprehensive anatomical map of the peripheral octopaminergic/tyraminergic system of *Drosophila melanogaster*. *Sci. Rep.*, **8**: 15314. doi:10.1038/s41598-018-33686-3

Peiffer, M. and Felton, G. W. (2014). Insights into the saliva of the Brown Marmorated Stink Bug *Halyomorpha halys* (Hemiptera: Pentatomidae). *PLoS ONE* **9**, e88483. doi:10.1371/journal.pone.0088483

Pezzi, M., Cultrera, R., Chicca, M. and Leis, M. (2015). Scanning electron microscopy investigations of third-instar larva of *Cordylobia rodhaini* (Diptera: Calliphoridae), an agent of furuncular myiasis. *J. Med. Entomol.* **52**, 368-374. doi:10.1093/jme/tjv022

Pezzi, M., Whitmore, D., Chicca, M., Semeraro, B., Brighi, F. and Leis, M. (2016). Ultrastructural morphology of the antenna and maxillary palp of *Sarcophaga tibialis* (Diptera: Sarcophagidae). *J. Med. Entomol.* **53**, 807-814. doi:10.1093/jme/tjw061

Poels, J., Suner, M. M., Needham, M., Torfs, H., De Rijck, J., De Loof, A., Dunbar, S. J. and Vanden Broeck, J. (2001). Functional expression of a locust tyramine receptor in murine erythroleukaemia cells. *Insect Mol. Biol.* **10**, 541-548. doi:10.1046/j.0962-1075.2001.00292.x

Reis, S. L., Mantello, A. G., Macedo, J. M., Gelfuso, E. A., da Silva, C. P., Fachin, A. L., Cardoso, A. M. and Beleboni, R. O. (2016). Typical monoterpenes as insecticides and repellents against stored grain pests. *Molecules* **21**, 258. doi:10.3390/molecules21030258

Rice, K. B., Bergh, C. J., Bergmann, E. J., Biddinger, D. J., Dieckhoff, C., Dively, G., Fraser, H., Gariepy, T., Hamilton, G., Haye, T. et al. (2014). Biology, ecology, and management of brown marmorated stink bug (Hemiptera: Pentatomidae). *J. Integr. Pest Manag.* **5**, 1-13. doi:10.1603/IPM14002

Riga, M., Deneck, S., Livadaras, I., Geibel, S., Nauen, R. and Vontas, J. (2019). Development of efficient RNAi in *Nezara viridula* for use in insecticide target discovery. *Arch. Insect Biochem. Physiol.* **103**, e21650. doi:10.1002/arch.21650

Roeder, T. (2005). Tyramine and octopamine: ruling behaviour and metabolism. *Annu. Rev. Entomol.* **50**, 447-477. doi:10.1146/annurev.ento.50.071803.130404

Roeder, T. (2020). The control of metabolic traits by octopamine and tyramine in invertebrates. *J. Exp. Biol.* **223**, jeb194282. doi:10.1242/jeb.194282

Roeder, T., Seifert, M., Kähler, C. and Gewecke, M. (2003). Tyramine and octopamine: antagonist modulators of behavior and metabolism. *Arch. Insect Biochem. Physiol.* **54**, 1-13. doi:10.1002/arch.10102

Romeis, J. and Widmer, F. (2020). Assessing the risk of topically applied dsRNA-based products to non-target arthropods. *Front. Plant Sci.* **11**, 679. doi:10.3389/fpls.2020.00679

Rotte, C., Krach, C., Balfanz, S., Baumann, A., Walz, B. and Blenau, W. (2009). Molecular characterization and localization of the first tyramine receptor of the American cockroach (*Periplaneta americana*). *Neuroscience* **162**, 1120-1133. doi:10.1016/j.neuroscience.2009.05.066

Rouhana, L., Weiss, J. A., Forsthoefel, D. J., Lee, H., King, R. S., Inoue, T., Shibata, N., Agata, K. and Newmark, P. A. (2013). RNA interference by feeding in vitro synthetized double-stranded RNA to planarians: methodology and dynamics. *Dev. Dyn.* **242**, 718-730. doi:10.1002/dvdy.23950

Saraswati, S., Fox, L. E., Soll, D. R. and Wu, C.-F. (2004). Tyramine and octopamine have opposite effects on the locomotion of *Drosophila* larvae. *J. Neurobiol.* **58**, 425-441. doi:10.1002/neu.10298

Saudou, F., Amlaiky, N., Plassat, J. L., Borrelli, E. and Hen, R. (1990). Cloning and characterization of a *Drosophila* tyramine receptor. *EMBO J.* **9**, 3611-3617. doi:10.1002/j.1460-2075.1990.tb07572.x

Schützler, N., Girwert, C., Hügli, I., Mohana, G., Roignant, J.-Y., Ryglewski, S. and Duch, C. (2019). Tyramine action on motoneuron excitability and adaptable tyramine/octopamine ratios adjust *Drosophila* locomotion to nutritional state. *Proc. Natl. Acad. Sci. USA* **116**, 3805-3810. doi:10.1073/pnas.1813554116

Sinakevitch, I. T., Daskalova, S. M. and Smith, B. H. (2017). The biogenic amine tyramine and its receptor (AmTyr1) in olfactory neuropils in the honeybee (*Apis mellifera*) brain. *Front. Syst. Neurosci.* **11**, 77. doi:10.3389/fnsys.2017.00077

Tanaka, N. K., Suzuki, E., Dye, L., Ejima, A. and Stopfer, M. (2012). Dye fills reveal additional olfactory tracts in the protocerebrum of wild-type *Drosophila*. *J. Comp. Neurol.* **520**, 4131-4140. doi:10.1002/cne.23149

Thamm, M., Scholl, C., Reim, T., Grübel, K., Möller, K., Rössler, W. and Scheiner, R. (2017). Neuronal distribution of tyramine and the tyramine receptor AmTAR1 in the honeybee brain. *J. Comp. Neurol.* **525**, 2615-2631. doi:10.1002/cne.24228

Toyama, M., Ihara, F. and Yaginuma, K. (2006). Formation of aggregations in adults of the brown marmorated stink bug, *Halyomorpha halys* (Stål) (Heteroptera: Pentatomidae): the role of antennae in short-range locations. *Appl. Entomol. Zool.* **41**, 309-315. doi:10.1303/aez.2006.309

Valentin, R. E., Nielsen, A. L., Wiman, N. G., Lee, D.-H. and Fonseca, D. M. (2017). Global invasion network of the brown marmorated stink bug, *Halyomorpha halys*. *Sci. Rep.* **7**, 9866. doi:10.1038/s41598-017-10315-z

Waterhouse, A., Bertoni, M., Bienert, S., Studer, G., Tauriello, G., Gumienny, R., Heer, F. T., de Beer, T. A. P., Rempfer, C., Bordoli, L. et al. (2018). SWISS-MODEL: homology modelling of protein structures and complexes. *Nucleic Acids Res.* **46**, 296-303. doi:10.1093/nar/gky427

Wu, S.-F., Xu, G., Qi, Y.-X., Xia, R.-Y., Huang, J. and Ye, G.-Y. (2014). Two splicing variants of a novel family of octopamine receptors with different signalling properties. *J. Neurochem.* **129**, 37-47. doi:10.1111/jnc.12526

Zacharuk, R. Y. (1985). Antennae and sensilla. In *Comprehensive Insect Physiology, Biochemistry and Pharmacology*, Vol. 6 (ed. G. A. Kerkut and L. I. Gilbert), pp. 1-69. Pergamon Press.

Zhao, Z. and McBride, C. S. (2020). Evolution of olfactory circuits in insects. *J. Comp. Physiol. A* **206**, 353-367. doi:10.1007/s00359-020-01399-6

Zhong, Z.-Z., Zhang, J.-P., Ren, L.-L., Tang, R., Zhang, H.-X., Chen, G.-H. and Zhang, F. (2017). Behavioral responses of the egg parasitoid *Trissolcus japonicus* to volatiles from adults of its stink bug host, *Halyomorpha halys*. *J. Pest Sci.* **90**, 1097-1105. doi:10.1007/s10340-017-0884-6

Zhong, Z.-Z., Tang, R., Zhang, J.-P., Yang, S.-Y., Chen, G.-H., He, K.-L., Wang, Z.-Y. and Zhang, F. (2018). Behavioral evidence and olfactory reception of a single alarm pheromone component in *Halyomorpha halys*. *Front. Physiol.* **9**, 1610. doi:10.3389/fphys.2018.01610

Zhukovskaya, M. I. and Polyanovsky, A. D. (2017). Biogenic amines in insect antennae. *Front. Syst. Neurosci.* **11**, e72785. doi:10.3389/fnsys.2017.00045

Supplementary Figure S1

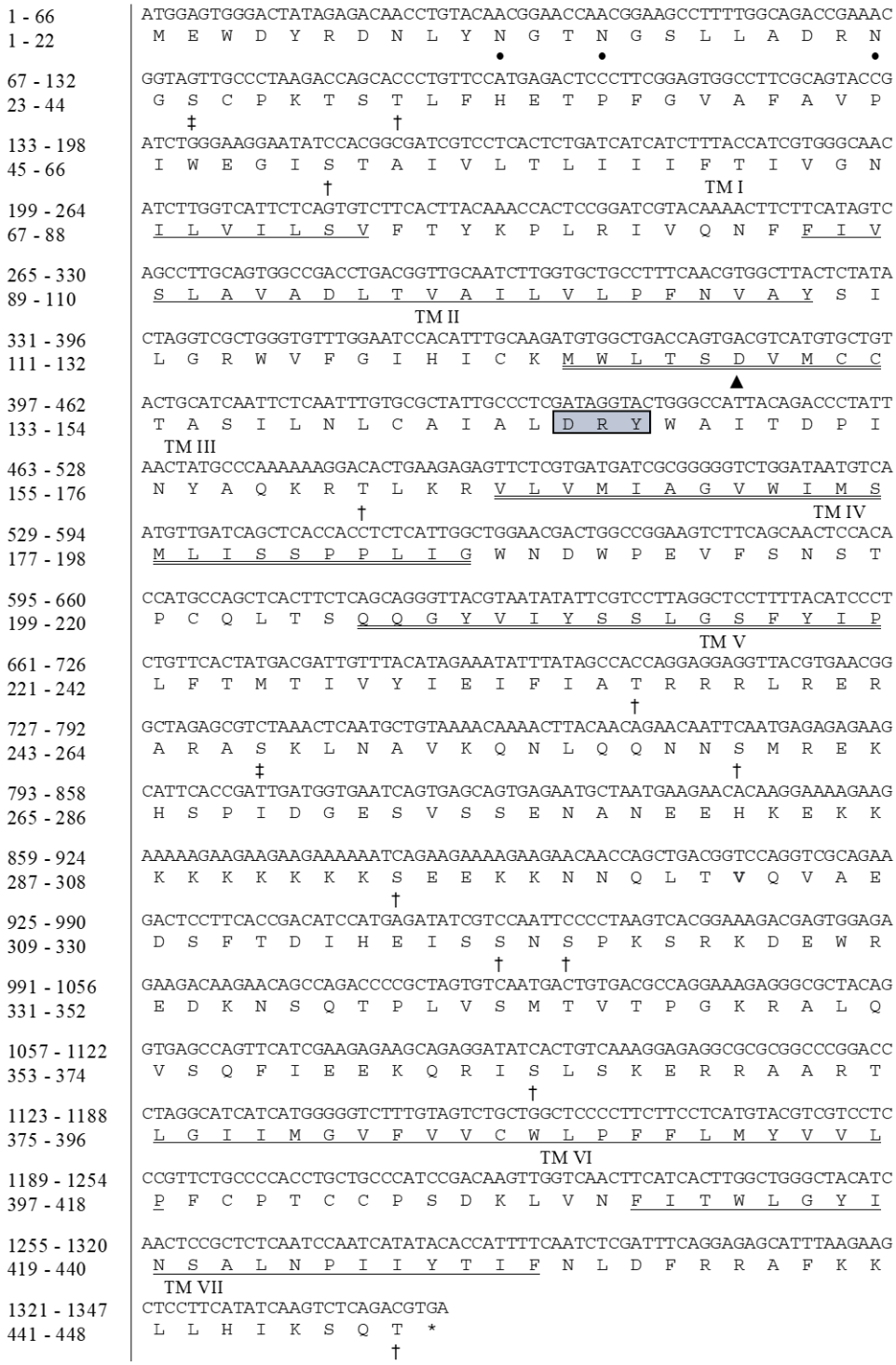

Figure S1. Nucleotide sequence of the TAR1 open reading frame cloned from *Halyomorpha halys* and deduced amino acid sequence. Prediction of the transmembrane segments (underlined and numbered from I to VII) was obtained with TMHMM v. 2.0 software. After the third transmembrane domain there is the DRY motif (highlighted with a box). Potential sites for N-linked glycosylation (predicted with NetNGlyc 1.0 server) are shown with a ● and potential sites for PKA or PKC phosphorylation (predicted with NetPhos 3.1 server) are shown with a † and a ‡ respectively.

Supplementary Figure S2

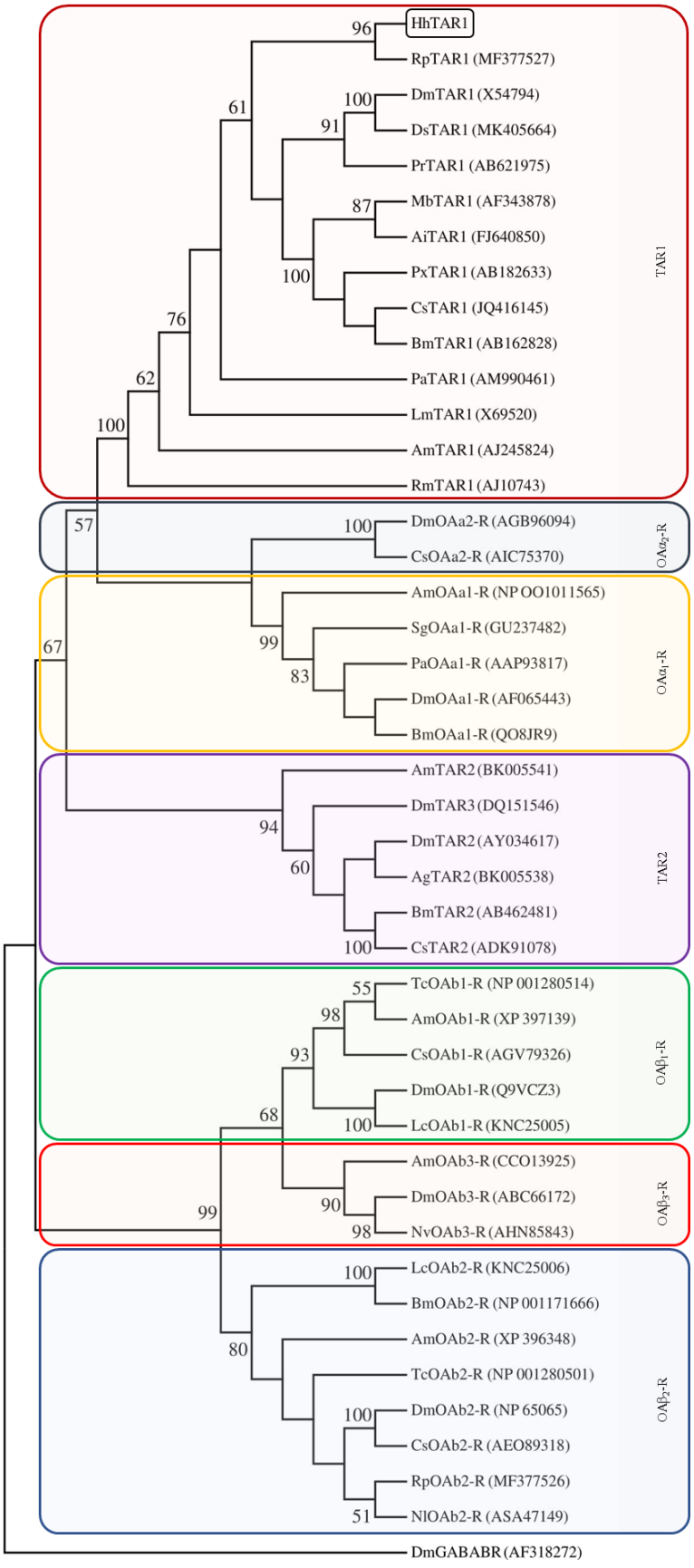

Figure S2. Phylogenetic relationships of HhTAR1 and other insect amine receptors resulting from neighbour joining analysis, using MEGA7. The values shown at the nodes of the branches are the percentage bootstrap support (1000 replications) for each branch. Alignment was performed using the amino acid sequences found in GenBank (accession number are indicated). *Drosophila melanogaster* GABA-B receptor (DmGABABR) was chosen as outgroup. Dm, *Drosophila melanogaster*; Ds, *Drosophila suzukii*; Pr, *Phormia regina*; Hh, *Halyomorpha halys*; Rp, *Rhodnius prolixus*; Px, *Papilio xuthus*; Cs, *Chilo suppressalis*; Bm, *Bombyx mori*; Ai, *Agnotis ipsilon*; Mb, *Mamestra brassicae*; Pa, *Periplaneta americana*; Lm, *Locusta migratoria*; Am, *Apis mellifera*; Rm, *Rhipicephalus microplus*; Sg, *Schistocerca gregaria*; Ag, *Anopheles gambiae*; Tc, *Tribolium castaneum*; Nv, *Nilaparvata lugens*; Lc, *Lucilia cuprina*; Nl, *Nilaparvata lugens*.

Supplementary Figure S3

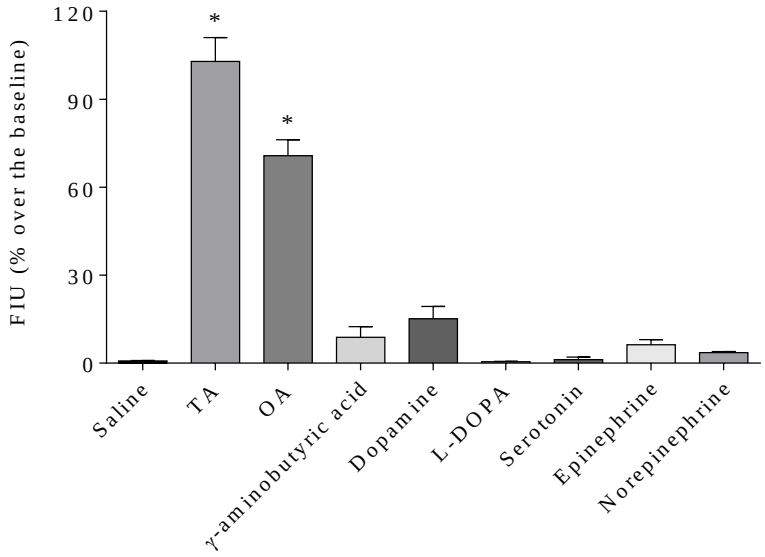

Figure S3. Effect of biogenic amines and γ-aminobutyric acid on the intracellular calcium release in HEK 293 stably expressing HhTAR1. All compounds were tested at 10^{-4} M. Data represent means ± SEM of three separate experiments performed in duplicate. * $p < 0.001$ vs saline according to one-way ANOVA followed by Dunnett's multiple comparison test.

Supplementary Figure S4

Figure S4. Image of dsRNA topically delivered on a *H. halys* 2nd instar nymph. The 2nd instar nymphs were collected 3 days post-ecdysis and placed on double-sided adhesive tape to avoid movements. One µl of the dsRNA solution was placed on the dorsal side of the abdomen. When the dsRNA solution was completely absorbed, the nymphs were put back in the nursery cage.

Supplementary Figure S5

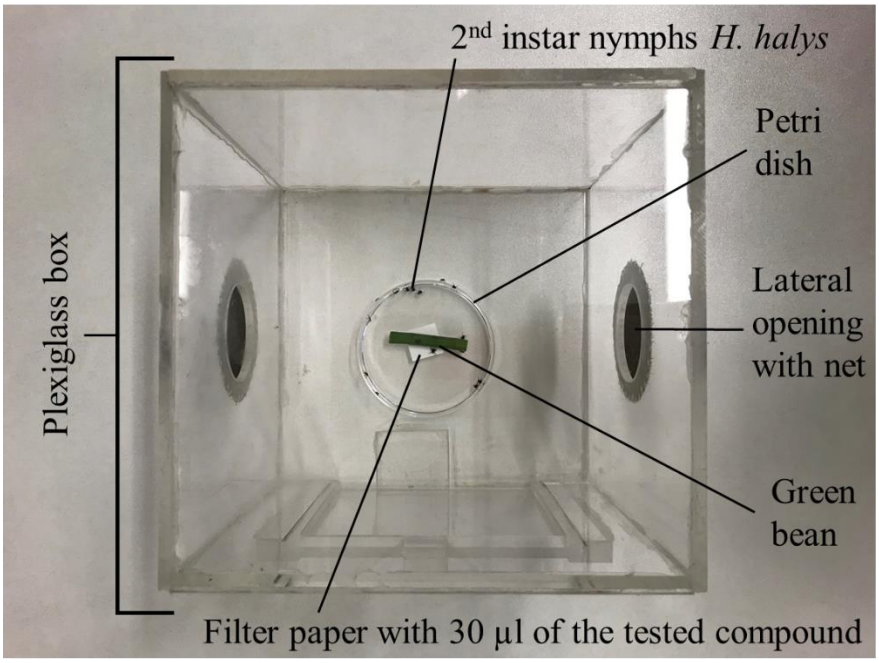

Figure S5. Arena set up for *H. halys* repellency assay.